

# UniPC: A Unified Predictor-Corrector Framework for Fast Sampling of Diffusion Models

Wenliang Zhao <sup>\*1</sup> Lujia Bai <sup>\*1</sup> Yongming Rao <sup>1</sup> Jie Zhou <sup>1</sup> Jiwen Lu <sup>1</sup>

## Abstract

Diffusion probabilistic models (DPMs) have demonstrated a very promising ability in high-resolution image synthesis. However, sampling from a pre-trained DPM usually requires hundreds of model evaluations, which is computationally expensive. Despite recent progress in designing high-order solvers for DPMs, there still exists room for further speedup, especially in extremely few steps (*e.g.*, 5~10 steps). Inspired by the predictor-corrector for ODE solvers, we develop a unified corrector (UniC) that can be applied after any existing DPM sampler to increase the order of accuracy without extra model evaluations, and derive a unified predictor (UniP) that supports arbitrary order as a byproduct. Combining UniP and UniC, we propose a unified predictor-corrector framework called UniPC for the fast sampling of DPMs, which has a unified analytical form for any order and can significantly improve the sampling quality over previous methods. We evaluate our methods through extensive experiments including both unconditional and conditional sampling using pixel-space and latent-space DPMs. Our UniPC can achieve 3.87 FID on CIFAR10 (unconditional) and 7.51 FID on ImageNet 256×256 (conditional) with only 10 function evaluations. Code is available at <https://github.com/wl-zhao/UniPC>.

## 1. Introduction

Diffusion probabilistic models (DPMs) (Sohl-Dickstein et al., 2015; Ho et al., 2020; Song et al., 2021b) have become the new prevailing generative models and have achieved competitive performance on many tasks including image synthesis (Dhariwal & Nichol, 2021; Rombach et al., 2022; Ho et al., 2020), video synthesis (Ho et al., 2022), text-to-image generation (Nichol et al., 2022; Rombach et al.,

<sup>\*</sup>Equal contribution <sup>1</sup>Tsinghua University. Correspondence to: Jiwen Lu <lujiwen@tsinghua.edu.cn>.

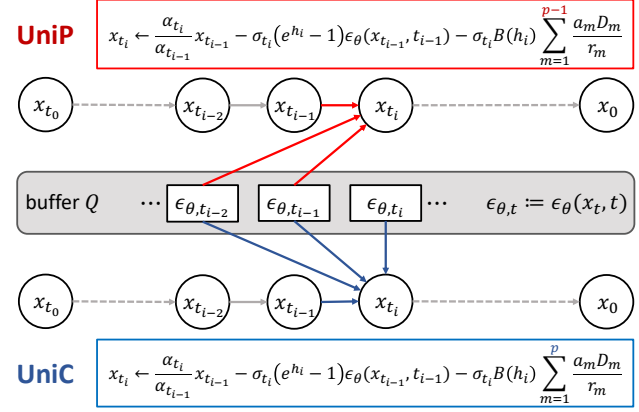


**Figure 1. The main idea of UniPC.** We provide an illustration of the multistep variant of our UniPC with noise prediction, where  $p = 2$ . As a predictor-corrector style fast sampler for DPMs, UniPC consists of UniP and UniC which share the same analytical form. Apart from only considering the output of  $\epsilon_{\theta}$  in previous timesteps, UniC can increase the order of accuracy by also leveraging the model output of the current timestep  $t_i$  to produce a corrected  $x_{t_i}$ , see Section 3 for details.

2022; Gu et al., 2022), voice synthesis (Chen et al., 2021), *etc.* Different from GANs (Goodfellow et al., 2014) and VAEs (Kingma & Welling, 2014), DPMs are trained to explicitly match the gradient of the data density (*i.e.*, score), which is more stable and less sensitive to hyper-parameters. However, the sampling of DPMs requires gradually performing denoising using the pre-trained model, starting from Gaussian noise. Thus generating high-quality visual content using DPMs usually needs hundreds of model evaluations (Ho et al., 2020) and is quite time-consuming. Therefore, it is of great importance to design fast samplers for DPMs to better deploy DPMs in downstream applications.

There are mainly two categories of existing fast samplers for DPMs, training-based methods and training-free methods. While training-based methods (Salimans & Ho, 2022; Nichol & Dhariwal, 2021; Watson et al., 2021) can achieve impressive sampling results in very few steps (*e.g.*, 4 steps in (Salimans & Ho, 2022)), they require an extra training stage, which makes it difficult to efficiently sample from an arbitrary off-the-shelf pre-trained DPM. On the other hand, training-free methods aim to accelerate the sampling from



**Figure 2. Qualitative comparisons between our UniPC and previous methods.** All images are generated by sampling from a DPM trained on ImageNet  $256 \times 256$  with only 7 number of function evaluations (NFE) and a classifier scale of 8.0. We show that our proposed UniPC can generate more plausible samples with more visual details compared with previous first-order sampler (Song et al., 2021a) and high-order samplers (Zhang & Chen, 2022; Lu et al., 2022b). Best viewed in color.

the general reverse process and are more flexible to be used in a wider range of applications including both unconditional sampling (Song et al., 2021a; Lu et al., 2022a) and conditional sampling (Lu et al., 2022b; Dhariwal & Nichol, 2021). However, the sampling performance of training-free methods with extremely few steps (*e.g.*,  $< 10$ ) has been rarely investigated and still has room for improvement.

In this paper, we propose a new framework for training-free fast sampling of DPMs called ***UniPC***, consisting of a corrector (UniC) and a predictor (UniP) that share a unified analytical form and support arbitrary orders. Inspired by the predictor-corrector methods in ODE solvers (Lambert et al., 1991), we develop a unified corrector (UniC) that can be applied after any existing DPM sampler to increase the order of accuracy, at the cost of no extra model evaluations. Specifically, UniC works by using the output of the model output  $\epsilon_\theta(\mathbf{x}_{t_i}, t_i)$  at the current timestep  $t_i$  to obtain a refined  $\mathbf{x}_{t_i}^c$ . Interestingly, we find that a unified predictor (UniP) can be derived by simply changing a hyperparameter in UniC. Different from previous fast solvers (Lu et al., 2022b;a; Zhang & Chen, 2022) that either have no higher-order (*e.g.*,  $> 3$ ) variants or have no explicit forms, our UniP and UniC support arbitrary orders with a unified analytical expression and are easy to implement. Since our UniC is method-agnostic, we combine UniP and UniC to obtain a new family of fast samplers called UniPC, which is suitable for both conditional sampling and unconditional sampling. Benefiting from the universal design, variants of UniPC (*e.g.*, singlestep/multistep, noise/data prediction) can be easily derived. An illustration of our method is shown in Figure 1, where we demonstrate a multistep variant of our UniPC with noise prediction.

We conduct extensive experiments with both pixel-space and latent-space DPMs to verify the effectiveness of the proposed UniPC. Our results show that UniPC performs

consistently better than previous state-of-the-art methods on both unconditional and conditional sampling tasks. Notably, UniPC can achieve 3.87 FID on CIFAR10 (unconditional) and 7.51 FID on ImageNet  $256 \times 256$  (conditional) with only 10 function evaluations. We also demonstrate that UniC can improve the sampling quality of several existing fast samplers significantly with very few NFE (number of function evaluations). Some qualitative comparisons are shown in Figure 2, where we observe that our UniPC can generate images with more visual details than other methods.

## 2. Background and Related Work

We review basic ideas of diffusion probabilistic models (DPMs), diffusion ordinary differential equations (ODEs), and the existing sampling methods.

### 2.1. Diffusion Probabilistic Models

For a random variable  $\mathbf{x}_0$  with an unknown distribution  $q_0(\mathbf{x}_0)$ , Diffusion Probabilistic Models (DPMs) (Sohl-Dickstein et al., 2015; Ho et al., 2020; Kingma et al., 2021) transit  $q_0(\mathbf{x}_0)$  at time 0 to a normal distribution  $q_T(\mathbf{x}_T) \approx \mathcal{N}(\mathbf{x}_T | \mathbf{0}, \tilde{\sigma}^2 \mathbf{I})$  at time  $T$  for some  $\tilde{\sigma} > 0$  by gradually adding Gaussian noise to the observation  $\mathbf{x}_0$ . For each time  $t \in [0, T]$ , and given  $\sigma_t, \alpha_t > 0$ , the Gaussian transition is

$$q_{t0}(\mathbf{x}_t | \mathbf{x}_0) = \mathcal{N}(\mathbf{x}_t | \alpha_t \mathbf{x}_0, \sigma_t^2 \mathbf{I}),$$

where  $\alpha_t^2 / \sigma_t^2$  (the *signal-to-noise-ratio* (SNR)) is strictly decreasing w.r.t.  $t$  (Kingma et al., 2021).

Let  $\epsilon_\theta(\mathbf{x}_t, t)$  denote the noise prediction model using data  $\mathbf{x}_t$  to predict the noise  $\epsilon$ , and the parameter  $\theta$  is obtain by minimizing

$$\mathbb{E}_{\mathbf{x}_0, \epsilon, t} [\omega(t) \|\epsilon_\theta(\mathbf{x}_t, t) - \epsilon\|_2^2],$$

where  $\mathbf{x}_0 \sim q_0(\mathbf{x}_0)$ ,  $t \in \mathcal{U}[0, T]$ , and the weight function  $\omega(t) > 0$ . Sampling from DPMs can be achieved by solving the following diffusion ODEs (Song et al., 2021b):

$$\frac{d\mathbf{x}_t}{dt} = f(t)\mathbf{x}_t + \frac{g^2(t)}{2\sigma_t}\epsilon_\theta(\mathbf{x}_t, t), t \in [0, T] \quad (1)$$

$$\mathbf{x}_T \sim \mathcal{N}(\mathbf{0}, \tilde{\sigma}^2 \mathbf{I}),$$

where  $f(t) = \frac{d \log \alpha_t}{dt}$ ,  $g^2(t) = \frac{d \sigma_t^2}{dt} - 2 \frac{d \log \alpha_t}{dt} \sigma_t^2$ .

## 2.2. Fast Sampling of DPMs

Fast samplers of DPMs can be either training-based (Salimans & Ho, 2022; Bao et al., 2022a; Watson et al., 2021) or training-free (Lu et al., 2022a;b; Zhang & Chen, 2022; Liu et al., 2022; Zhang et al., 2022). Training-based samplers require further training costs while training-free methods directly use the original information without re-training and are easy to implement in conditional sampling. The essence of training-free samplers is solving stochastic differential equations (SDEs) (Ho et al., 2020; Song et al., 2021b; Bao et al., 2022b; Zhang et al., 2022) or ODEs (Lu et al., 2022b; Zhang & Chen, 2022; Liu et al., 2022; Song et al., 2021a; Lu et al., 2022a). Other fast sampling methods include modifying DPMs (Dockhorn et al., 2022) and the combination with GANs (Xiao et al., 2022; Wang et al., 2022).

Among others, samplers solving diffusion ODEs are found to converge faster for the purpose of sampling DPMs (Song et al., 2021a;b). Recent works (Zhang & Chen, 2022; Lu et al., 2022a;b) show that ODE solvers built on exponential integrators (Hochbruck & Ostermann, 2010) are shown to have faster convergence than those directly solving the unconditional diffusion ODE (1). The solution  $\mathbf{x}_t$  of the diffusion ODE given the initial value  $\mathbf{x}_s$  can be analytically computed as (Lu et al., 2022a):

$$\mathbf{x}_t = \frac{\alpha_t}{\alpha_s} \mathbf{x}_s - \alpha_t \int_{\lambda_s}^{\lambda_t} e^{-\lambda} \hat{\epsilon}_\theta(\hat{\mathbf{x}}_\lambda, \lambda) d\lambda, \quad (2)$$

where we use the notation  $\hat{\epsilon}_\theta$  and  $\hat{\mathbf{x}}_\lambda$  to denote changing from the domain of time ( $t$ ) to the domain of half log-SNR( $\lambda$ ), i.e.,  $\hat{\mathbf{x}}_\lambda := \mathbf{x}_{t_\lambda(\lambda)}$  and  $\hat{\epsilon}_\theta(\cdot, \lambda) := \epsilon_\theta(\cdot, t_\lambda(\lambda))$ .

Although many high-order solvers are proposed, existing solvers of diffusion ODEs can be explicitly computed for orders not greater than 3 (Lu et al., 2022a;b; Zhang & Chen, 2022; Liu et al., 2022), due to the lack of analytical forms.

## 3. A Unified Predictor-Corrector Solver

In this section, we propose a unified predictor-corrector solver of DPMs called UniPC, consisting of UniP and UniC. Our UniPC is unified in mainly two aspects: 1) the predictor (UniP) and the corrector (UniC) share the same analytical form; 2) UniP supports arbitrary order and UniC can be

applied after off-the-shelf fast samplers of DPMs to increase the order of accuracy.

### 3.1. The Unified Corrector UniC- $p$

Inspired by the idea of predictor-corrector methods that have been widely applied in solving ODEs numerically such as the Modified-Euler method (Griffiths & Higham, 2010), we propose to improve the initial solutions using previous  $p$  points and the current point. Suppose we have  $\text{Solver-}p$ , a solver of order of accuracy  $p$ , which computes a sequence  $\{\tilde{\mathbf{x}}_{t_i}\}_{i=0}^M$ . Define  $h_i = \lambda_{t_i} - \lambda_{t_{i-1}}$ . For an increasing non-zero sequence  $r_1 < r_2 < \dots < r_p = 1$ , let  $\lambda_{s_m} = r_m h_i + \lambda_{t_{i-1}}$ ,  $s_m = t_\lambda(\lambda_{s_m})$ ,  $m = 1, \dots, p-1$ ,  $\lambda_{s_p} = \lambda_{t_i}$ ,  $s_p = t_i$ . We formulate the unified corrector (UniC- $p$ ) as

$$\begin{aligned} \tilde{\mathbf{x}}_{t_i}^c &= \frac{\alpha_{t_i}}{\alpha_{t_{i-1}}} \tilde{\mathbf{x}}_{t_{i-1}} - \sigma_{t_i} (e^{h_i} - 1) \epsilon_\theta(\tilde{\mathbf{x}}_{t_{i-1}}, t_{i-1}) \\ &\quad - \sigma_{t_i} B(h_i) \sum_{m=1}^p \frac{a_m}{r_m} D_m, \end{aligned} \quad (3)$$

where  $B(h)$  is some function of  $h$  such that  $B(h) = \mathcal{O}(h)$  and  $B(h) \neq 0$ , and

$$D_m = \epsilon_\theta(\tilde{\mathbf{x}}_{s_m}, s_m) - \epsilon_\theta(\tilde{\mathbf{x}}_{t_{i-1}}, t_{i-1}). \quad (4)$$

The traditional approach to determine  $a_m$  is to use the classical Taylor series expansions of  $\mathbf{x}_t$ . However, due to the semilinear structure, the nonlinearity of  $\epsilon_\theta$  of (3) and the exponential integration in the ‘‘variation of constants’’ formula (Lambert et al., 1991) of solving (1), such approach would be intractable. Alternatively, we derive  $a_m$  by Taylor expansion of  $\epsilon_\theta$  in (3) and matching coefficients in the insightful expansion of (Lu et al., 2022a) of (2), i.e.,

$$\begin{aligned} \mathbf{x}_{t_i} &= \frac{\alpha_{t_i}}{\alpha_{t_{i-1}}} \mathbf{x}_{t_{i-1}} - \sigma_{t_i} (e^{h_i} - 1) \epsilon_\theta(\mathbf{x}_{t_{i-1}}, t_{i-1}) \\ &\quad - \sigma_{t_i} \sum_{k=1}^p h_i^{k+1} \varphi_{k+1}(h_i) \hat{\epsilon}_\theta^{(k)}(\hat{\mathbf{x}}_{\lambda_{t_{i-1}}}, \lambda_{t_{i-1}}) + \mathcal{O}(h_i^{p+2}). \end{aligned}$$

where the functions  $\varphi_k(h)$  can be analytically computed (Hochbruck & Ostermann, 2005) and circumvent the complicated evaluation of exponential integration. In the following theorem, we show that UniC- $p$  has an order of accuracy  $p+1$ . The proof is in Appendix E.3. The algorithm is given in Algorithm 1.

**Theorem 3.1** (The Order of Accuracy of UniC- $p$ ). *For any non-zero sequence  $\{r_i\}_{i=1}^p$  and  $h > 0$  define*

$$\mathbf{R}_p(h) = \begin{pmatrix} 1 & 1 & \cdots & 1 \\ r_1 h & r_2 h & \cdots & r_p h \\ \cdots & \cdots & \cdots & \cdots \\ (r_1 h)^{p-1} & (r_2 h)^{p-1} & \cdots & (r_p h)^{p-1} \end{pmatrix}.$$

Let  $\phi_p(h) = (\phi_1(h), \dots, \phi_p(h))^\top$  with

$$\phi_n(h) = h^n n! \varphi_{n+1}(h),$$

**Algorithm 1** UniC- $p$ 

**Require:**  $\{r_i\}_{i=1}^{p-1}$ , noise prediction model  $\epsilon_\theta$ , any  $p$ -order solver `Solver-p`, an estimate at  $t_{i-1}$  namely  $\tilde{\mathbf{x}}_{t_{i-1}}$ , and a buffer  $Q$  containing previous outputs of  $\epsilon_\theta$ .  
 $h_i \leftarrow \lambda_{t_i} - \lambda_{t_{i-1}}$ ,  $r_p \leftarrow 1$ ,  $\tilde{\mathbf{x}}_{t_i} \leftarrow \text{Solver-p}(\tilde{\mathbf{x}}_{t_{i-1}}, Q)$   
**for**  $m = 1$  **to**  $p$  **do**  
     $s_m \leftarrow t_\lambda(r_m h_i + \lambda_{t_{i-1}})$   
     $D_m \leftarrow \epsilon_\theta(\tilde{\mathbf{x}}_{s_m}, s_m) - \epsilon_\theta(\tilde{\mathbf{x}}_{t_{i-1}}, t_{i-1})$   
**end for**  
Compute  $\mathbf{a}_p \leftarrow \mathbf{R}_p^{-1}(h_i)\phi_p(h_i)/B(h_i)$ , where  $\mathbf{R}_p$  and  $\phi_p$  are as defined in Theorem 3.1  
 $\tilde{\mathbf{x}}_{t_i}^c \leftarrow \frac{\alpha_{t_i}}{\alpha_{t_{i-1}}} \tilde{\mathbf{x}}_{t_{i-1}} - \sigma_{t_i}(e^{h_i} - 1)\epsilon_\theta(\tilde{\mathbf{x}}_{t_{i-1}}, t_{i-1})$   
 $- \sigma_{t_i}B(h_i) \sum_{m=1}^p a_m D_m / r_m$   
 $Q \xleftarrow{\text{buffer}} \epsilon_\theta(\tilde{\mathbf{x}}_{t_i}, t_i)$   
**return:**  $\tilde{\mathbf{x}}_{t_i}^c$

where  $\varphi_n(h)$  is defined by the recursive relation (Hochbruck & Ostermann, 2005):

$$\varphi_{n+1}(h) = \frac{\varphi_n(h) - 1/n!}{h}, \quad \varphi_0(h) = e^h.$$

For an increasing sequence  $r_1 < r_2 < \dots < r_p = 1$ , suppose  $\mathbf{a}_p := (a_1, \dots, a_p)^\top$  satisfies,

$$|\mathbf{R}_p(h_i)\mathbf{a}_p B(h_i) - \phi_p(h_i)| = \mathcal{O}(h_i^{p+1}), \quad (5)$$

where  $|\cdot|$  denotes the  $l_1$  norm for matrix. Then, under regularity conditions in Appendix E.2, UniC- $p$  of (3) will have  $(p+1)$ -th order of accuracy.

The monotonicity of  $\{r_i\}_{i=1}^p$  ensures the invertibility of the Vandermonde matrix  $\mathbf{R}_p$ . Therefore, we can take  $\mathbf{a}_p = \mathbf{R}_p^{-1}(h_i)\phi_p(h_i)/B(h_i)$  as the coefficient vector for (3) for simplicity, where  $B(h)$  can be any function of  $h$  such that  $B(h) = \mathcal{O}(h)$ , for example  $B_1(h) = h$ ,  $B_2(h) = e^h - 1$ .

### 3.2. The Unified Predictor UniP- $p$

The viewpoint of the predictor-corrector method also enables us to investigate explicit formulations of high-order predictors in a systematic manner. We find that the order of accuracy of UniC does not depend on the specific choice of the sequence  $\{r_i\}_{i=1}^p$ , which motivates us to design  $p$ -order unified predictor (UniP- $p$ ) which only leverages the previous  $p$  data points by excluding  $D_p$  in (3) since  $D_p$  involves  $\tilde{\mathbf{x}}_{t_i}$ . The order of accuracy is guaranteed by the following corollary.

**Corollary 3.2** (The Order of Accuracy of UniP- $p$ ). *For an increasing sequence  $r_1 < r_2 < \dots < r_{p-1} < 1$ , the solver given in (3) dropping the term  $D_p$  and using coefficients that satisfies*

$$|\mathbf{R}_{p-1}(h_i)\mathbf{a}_{p-1} B(h_i) - \phi_{p-1}(h_i)| = \mathcal{O}(h_i^p) \quad (6)$$

**Algorithm 2** UniP- $p$ 

**Require:**  $\{r_i\}_{i=1}^{p-1}$ , noise prediction model  $\epsilon_\theta$ , an estimate at  $t_{i-1}$  namely  $\tilde{\mathbf{x}}_{t_{i-1}}$ , and a buffer  $Q$  containing previous outputs of  $\epsilon_\theta$ .  
 $h_i \leftarrow \lambda_{t_i} - \lambda_{t_{i-1}}$   
**for**  $m = 1$  **to**  $p-1$  **do**  
     $s_m \leftarrow t_\lambda(r_m h_i + \lambda_{t_{i-1}})$   
     $D_m \leftarrow \epsilon_\theta(\tilde{\mathbf{x}}_{s_m}, s_m) - \epsilon_\theta(\tilde{\mathbf{x}}_{t_{i-1}}, t_{i-1})$   
**end for**  
Compute  $\mathbf{a}_{p-1} \leftarrow \mathbf{R}_{p-1}^{-1}(h_i)\phi_{p-1}(h_i)/B(h_i)$ , where  $\mathbf{R}_{p-1}$  and  $\phi_{p-1}$  are as defined in Theorem 3.1  
 $\tilde{\mathbf{x}}_{t_i} \leftarrow \frac{\alpha_{t_i}}{\alpha_{t_{i-1}}} \tilde{\mathbf{x}}_{t_{i-1}} - \sigma_{t_i}(e^{h_i} - 1)\epsilon_\theta(\tilde{\mathbf{x}}_{t_{i-1}}, t_{i-1})$   
 $- \sigma_{t_i}B(h_i) \sum_{m=1}^{p-1} a_m D_m / r_m$   
 $Q \xleftarrow{\text{buffer}} \epsilon_\theta(\tilde{\mathbf{x}}_{t_i}, t_i)$   
**return:**  $\tilde{\mathbf{x}}_{t_i}$

has  $p$ -th order of accuracy.

Due to the unified form of UniP and UniC, we can use UniP- $p$  as the implementation of the `Solver-p` in UniC- $p$  to obtain a new family of solvers called UniPC- $p$ . Theorem 3.1 and Corollary 3.2 ensure that UniPC- $p$  can achieve  $(p+1)$ -th order of accuracy. Moreover, under additional regularity conditions in Appendix D, based on Theorem 3.1 and Corollary 3.2, we show that the order of convergence of UniPC- $p$  reaches  $p+1$  (see Appendix D).

### 3.3. Comparison with Existing Methods

Here we discuss the connection and the difference between UniPC and previous methods. When  $p = 1$ , UniP will reduce to DDIM (Song et al., 2021a):

$$\tilde{\mathbf{x}}_{t_i} = \frac{\alpha_{t_i}}{\alpha_{t_{i-1}}} \tilde{\mathbf{x}}_{t_{i-1}} - \sigma_{t_i}(e^{h_i} - 1)\epsilon_\theta(\tilde{\mathbf{x}}_{t_{i-1}}, t_{i-1}),$$

which takes the advantage of the semi-linearity of diffusion ODEs and surpasses traditional Euler methods. Motivated by linear multistep approaches, PNDM (Liu et al., 2022) proposes to use pseudo numerical methods for DDIM, while our UniPC makes use of information in the ODE solution (2) and is specially designed for diffusion ODEs. DEIS (Zhang & Chen, 2022) is built on exponential integrators in the time domain, where the integral cannot be analytically computed and explicit formulae for high-order solvers cannot be derived. By using the half log-SNR  $\lambda$  (Lu et al., 2022a;b), it is shown that the application of integration-by-parts can simplify the integration of (2) and leads to explicit expansion of  $\mathbf{x}_t$ . DPM-Solver-2 (Lu et al., 2022a) lies in our UniPC framework as UniP-2 with  $B(h) = e^h - 1$ . We find through our numerical analysis that  $B(h)$  can be any non-degenerate function such that  $B(h) = \mathcal{O}(h)$ . Furthermore, DPM-Solver does not admit unified forms even for

orders smaller than 3, which adds to the challenge of obtaining algorithms for higher orders. In contrast, our UniPC exploits the structure of exponential integrators w.r.t. half log-SNR and admits not only simple and analytical solutions for efficient computation but also unified formulations for easy implementation of any order.

### 3.4. Implementation

By setting  $r_m = (\lambda_{t_{i-m-1}} - \lambda_{t_i})/h_i$ ,  $m = 1, \dots, p-1$ , the UniPC- $p$  updates in a multistep manner, which reuses the previous evaluation results and proves to be empirically more efficient, especially for limited steps of model evaluation (Griffiths & Higham, 2010; Lu et al., 2022b), while singlestep methods might incur higher computation cost per step. Therefore, we use multistep UniPC in our experiments by default. The detailed algorithms for multistep UniPC and the proof of convergence can be found in Appendix B. For UniPC, the choices of  $\{r_i\}_{i=1}^{p-1}$  determine different updating methods. If all the values are in  $(0, 1]$ , the UniPC will switch to singlestep. Notably, we find in experiments that our UniC consistently improves different updating methods. Besides, we find UniP-2 (6) and UniC-1 (5) degenerate to a simple equation where only a single  $a_1$  is unknown, where we find  $a_1 = 0.5$  can be a solution for both  $B_1(h)$  and  $B_2(h)$  (see Appendix F) independent of  $h$ . In Appendix C, we provide another variant of UniPC called UniPC<sub>v</sub> where the coefficients do not depend on  $h$  for arbitrary order  $p$ .

In the conditional inference, guided sampling (Ho & Salimans, 2021; Dhariwal & Nichol, 2021) is often employed. Recent works (Saharia et al., 2022; Lu et al., 2022b) find that thresholding data prediction models can boost the sampling quality and mitigate the problem of train-test mismatch. Our framework of UniPC can be easily adapted to the data prediction model, see Appendix A for algorithms and theoretical analysis. The detailed algorithms for multistep UniPC for data prediction are in Appendix B. Hence, UniPC with data prediction can achieve fast conditional sampling in extremely few steps through the dynamic thresholding.

## 4. Experiments

In this section, we show that our UniPC can significantly improve the sampling quality in very few steps through extensive experiments. Specifically, we perform experiments on both unconditional sampling and conditional sampling tasks and compare our UniPC with previous state-of-the-art methods. Since we focus on the fast sampling of diffusion models with few steps, we compare the sampling quality of different methods with 5~10 number of function evaluations (NFE). Our experiments cover a wide range of datasets, where the image resolution ranges from  $32 \times 32$  to  $256 \times 256$ . Apart from the standard image-space diffusion models (Song et al., 2021b; Dhariwal & Nichol, 2021), we

also conduct experiments on the recent prevailing stable-diffusion (Rombach et al., 2022) trained on latent space. We will first present our main results in Section 4.1 and then provide a detailed analysis in Section 4.2.

### 4.1. Main Results

We start by showing the effectiveness of our UniPC on both unconditional sampling and conditional sampling tasks, with extremely few model evaluations (5~10 NFE). For the sake of clarity, we only show the results of our UniPC and two previous representative methods DDIM (Song et al., 2021a) and DPM-Solver++ (Lu et al., 2022b). We have also conducted experiments with other methods including DPM-Solver (Lu et al., 2022a), DEIS (Zhang & Chen, 2022), and PNDM (Liu et al., 2022). However, since some of these methods perform very unstable in few-step sampling, we leave their results in Section 4.2 and Appendix G.

**Unconditional sampling.** We first compare the unconditional sampling quality of different methods on CIFAR10 (Krizhevsky et al., 2009), FFHQ (Karras et al., 2019), and LSUN Bedroom (Yu et al., 2015). The pre-trained diffusion models are from (Song et al., 2021b) and (Rombach et al., 2022), including both pixel-space and latent-space diffusion models. The results are shown in Figure 3, where we compare our UniPC with two previous representative methods DDIM (Song et al., 2021a) and DPM-Solver++ (Lu et al., 2022b). For DPM-Solver++, we use the multistep 3-order version due to its better performance. For UniPC, we use a combination of UniP-3 and UniC-3, thus the order of accuracy is 4. As shown in Figure 4, we find that our UniPC consistently achieves better sampling quality than DDIM and DPM-Solver++ on different datasets, especially with fewer NFE. Notably, when NFE=5, our UniPC achieves better FID than DPM-Solver++ by 6.0, 5.9, and 8.5 on CIFAR10, LSUN Bedroom, and FFHQ, respectively. These results clearly demonstrate that our UniPC can effectively improve the unconditional sampling quality with few function evaluations.

**Conditional sampling.** Conditional sampling is more useful since it allows user-defined input to control the synthesized image. To evaluate the conditional sampling performance of our UniPC, we conduct experiments on two widely used guided sampling settings, including classifier guidance and classifier-free guidance. For classifier guidance, we use the pixel-space diffusion model trained on ImageNet  $256 \times 256$  (Deng et al., 2009) provided by (Dhariwal & Nichol, 2021). Following DPM-Solver++, we use dynamic thresholding (Saharia et al., 2022) to mitigate the gap between training and testing. The results are shown in Figure 4a and 4b, where we compare our UniPC with DDIM (Song et al., 2021a) and DPM-Solver++ (Lu et al., 2022b) under different guidance scale ( $s = 8.0/4.0$ ). For

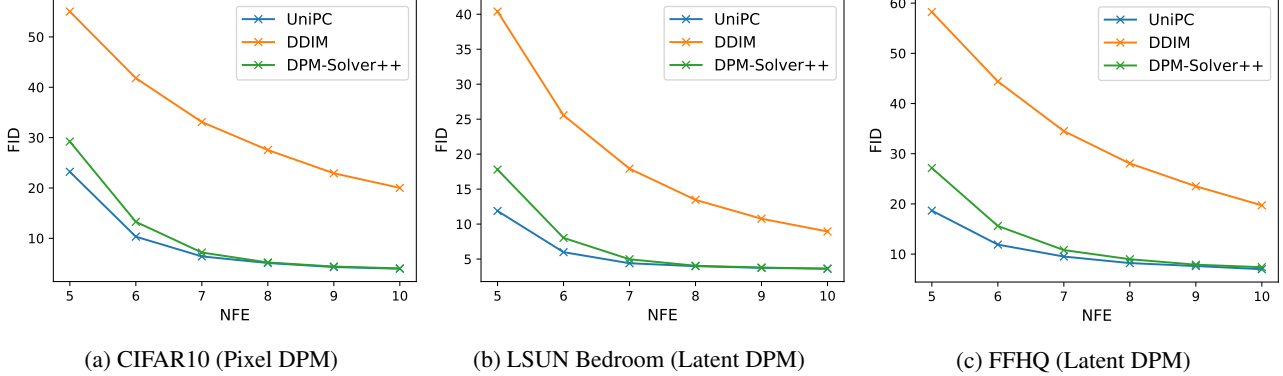


**Figure 3. Unconditional sampling results.** We compare our UniPC with DDIM (Song et al., 2021a) and DPM-Solver++ (Lu et al., 2022a) on CIFAR10, LSUN Bedroom, and FFHQ. We report the  $\text{FID}_{\downarrow}$  of the methods with different numbers of function evaluations (NFE). Experimental results demonstrate that our method is consistently better than previous ones on both pixel-space DPMs and latent-space DPMs, especially with extremely few steps. For  $\text{NFE} > 7$ , we recommend referring to Table 6-8 in Appendix G.

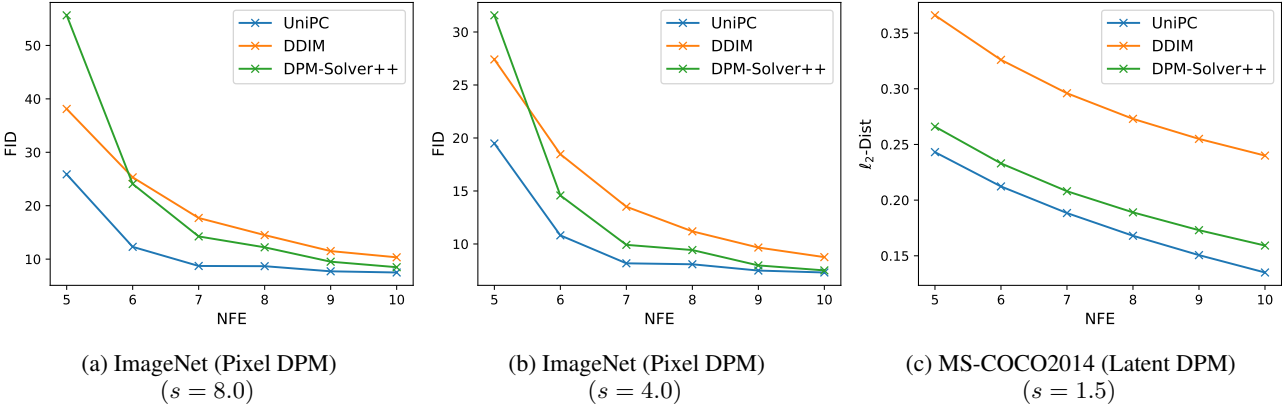


**Figure 4. Conditional sampling results.** (a)(b) We compare the sample quality measured by  $\text{FID}_{\downarrow}$  on ImageNet  $256 \times 256$  with guidance scale  $s = 8.0/4.0$ ; (c) We adopt the text-to-image model provided by stable-diffusion (Rombach et al., 2022) to compare the convergence error, which is measured by the  $l_2$  distance between the results of different methods and 1000-step DDIM. We show that our method outperforms previous ones with various guidance scales and NFE.

DPM-Solver++, we use the multistep 2-order version (2M), which achieves the best results according to the original paper. For our UniPC, we use UniP-2 and UniC-2. It can be seen that our UniPC generates samples with better quality and converges rather faster than other methods. For classifier-free guidance, we adopt the latent-space diffusion model provided by stable-diffusion (Rombach et al., 2022) and set the guidance scale as 1.5 following their original paper. To obtain the input texts, we randomly sample 10K captions from MS-COCO2014 validation dataset (Lin et al., 2014). As discussed in (Lu et al., 2022b), the FID of the text-to-image saturates in  $< 10$  steps, possibly because the powerful decoder can generate good image samples from non-converged latent codes. Therefore, to examine how fast a method converges, we follow (Lu et al., 2022b) to compute the  $l_2$ -distance between the generated latent code  $\mathbf{x}_0$  and the true solution  $\mathbf{x}_0^*$  (obtained by running a 999-step DDIM), *i.e.*,  $\|\mathbf{x}_0 - \mathbf{x}_0^*\|_2 / \sqrt{D}$ , where  $D$  is the dimension

of the latent code. For each text input, we use the same initial value  $\mathbf{x}_T^*$  sampled from Gaussian distribution for all the compared methods. It can be seen in Figure 4c that our UniPC consistently has a lower  $l_2$ -distance than DPM-Solver++ and DDIM, which indicates that UniPC converges faster in guided sampling.

## 4.2. Analysis

In this section, we will provide more detailed analyses to further evaluate the effectiveness of UniPC.

**Ablation on the choice of  $B(h)$ .** In Section 3, we mentioned that  $B(h)$  is set to be any non-zero function of  $h$  that satisfies  $B(h) = \mathcal{O}(h)$ . We now investigate how the choice of  $B(h)$  would affect the performance of our UniPC. Specifically, we test two simple forms:  $B_1(h) = h$  and  $B_2(h) = e^h - 1$  and the results are summarized in Table 1, where we also provide the performance of DPM-

**Table 1. Ablation on the choice of  $B(h)$ .** We investigate how the choice of  $B(h)$  affects the performance of our UniPC (measured by  $\text{FID} \downarrow$ ). Apart from the results of two implementations of  $B(h)$ , we also provide the performance of DPM-Solver++ (Lu et al., 2022b) for comparison. We show that while the UniPC with both the two forms of  $B(h)$  outperforms DPM-Solver++,  $B_1(h)$  performs better at fewer sampling steps.

Sampling Method	NFE			
	5	6	8	10
<i>CIFAR10, Pixel-space DPM</i>				
DPM-Solver++ (Lu et al.)	29.22	13.28	5.21	4.03
UniPC ( $B_1(h) = h$ )	<b>23.22</b>	<b>10.33</b>	<b>5.10</b>	3.97
UniPC ( $B_2(h) = e^h - 1$ )	26.20	11.48	5.11	<b>3.87</b>
<i>LSUN Bedroom, Latent-space DPM</i>				
DPM-Solver++ (Lu et al.)	17.79	8.03	4.04	3.63
UniPC ( $B_1(h) = h$ )	<b>11.88</b>	<b>5.99</b>	3.98	3.62
UniPC ( $B_2(h) = e^h - 1$ )	13.60	6.44	<b>3.91</b>	<b>3.54</b>
<i>FFHQ, Latent-space DPM</i>				
DPM-Solver++ (Lu et al.)	27.15	15.60	8.98	7.39
UniPC ( $B_1(h) = h$ )	<b>18.66</b>	<b>11.89</b>	<b>8.21</b>	<b>6.99</b>
UniPC ( $B_2(h) = e^h - 1$ )	21.66	13.21	8.63	7.20

Solver++ (Lu et al., 2022b) for reference. We show that UniPC with either implementation of  $B(h)$  can outperform DPM-Solver++. When the NFE is extremely small (5~6), we observe that  $B_1(h)$  consistently outperforms  $B_2(h)$  by 1~3 in FID. On the other hand, as the NFE increases, the performance of  $B_2(h)$  catches up and even surpasses  $B_1(h)$  in some experiments (e.g., on CIFAR10 and LSUN Bedroom). As for the guided sampling, we find  $B_1(h)$  is worse than  $B_2(h)$  consistently (see Appendix G for detailed results and discussions). These results also inspire us that our UniPC can be further improved by designing better  $B(h)$ , which we leave to future work.

**UniC for any order solver.** As shown in Algorithm 1, our UniC- $p$  can be applied after any  $p$ -order solver to increase the order of accuracy. To verify this, we perform experiments on a wide range of solvers. The existing solvers for DPM can be roughly categorized by the orders or the updating method (*i.e.*, singlestep or multistep). Since DPM-Solver++ (Lu et al., 2022b) by design has both singlestep and multistep variants of 1~3 orders, we apply our UniC to different versions of DPM-Solver++ to see whether UniC can bring improvements. The results are reported in Table 2, where the sampling quality is measured by  $\text{FID} \downarrow$  on CIFAR10 by sampling from a pixel-space DPM (Song et al., 2021b). We also provide the order of accuracy of each baseline method without/with our UniC. Apart from the DDIM (Song et al., 2021a), which can be also viewed as 1-order singlestep DPM-Solver++, we consider another 3 variants of DPM-Solver++ including 2-order multistep (2M), 3-order singlestep (3S) and 3-order multistep (3M). It can be found that our UniC can increase the order of accu-

**Table 2. Applying UniC to any solvers.** We demonstrate that our UniC can be a plug-and-play component to boost the performance of a wide range of solvers, including both singlestep and multistep solvers with different orders. The sampling quality is measured by  $\text{FID} \downarrow$  on the CIFAR10 dataset.

Sampling Method	Order	NFE			
		5	6	8	10
DDIM (Song et al.)	1	55.04	41.81	27.54	20.02
+ UniC (Ours)	2	47.22	33.70	19.20	12.77
DPM-Solver++(2M) (Lu et al.)	2	33.86	21.12	10.24	6.83
+ UniC (Ours)	3	31.23	17.96	8.09	5.51
DPM-Solver++ (3S) (Lu et al.)	3	51.49	38.83	11.98	6.46
+ UniC (Ours)	4	50.62	24.59	10.32	5.50
DPM-Solver++(3M) (Lu et al.)	3	29.22	13.28	5.21	4.03
+ UniC (Ours)	4	25.50	11.72	5.04	3.90

**Table 3. Exploring the upper bound of UniC.** We compare the performance of UniC and UniC-oracle by applying them to the DPM Solver++. Note that the NFE of UniC-oracle is twice the corresponding number of sampling steps. We show UniC-oracle can significantly improve the sampling quality over the baseline methods, indicating that UniC still has room for improvement.

Sampling Method	Sampling Steps			
	5	6	8	10
<i>LSUN Bedroom, Latent-space DPM</i>				
DPM Solver++ (Lu et al.)	17.79	8.03	4.04	3.63
+ UniC	13.79	6.53	3.98	3.52
+ UniC-oracle	6.06	4.39	3.46	3.22
<i>FFHQ, Latent-space DPM</i>				
DPM Solver++ (Lu et al.)	27.15	15.60	8.98	7.39
+ UniC	21.73	13.38	8.67	7.22
+ UniC-oracle	15.29	11.25	8.33	7.03

racy of the baseline methods by 1 and consistently improve the sampling quality for the solvers with different updating methods and orders.

**Exploring the upper bound of UniC.** According to Algorithm 1, our UniC works by leveraging the rough prediction  $\tilde{x}_{t_i}$  as another data point to perform correction and increase the order of accuracy. The correction procedure requires us to compute the model output at  $t_i$ , *i.e.*,  $\epsilon_\theta(\tilde{x}_{t_i}, t_i)$ . Note that to make sure there is no extra NFE, we directly feed  $\epsilon_\theta(\tilde{x}_{t_i}, t_i)$  to the next updating step instead of re-computing a  $\epsilon_\theta(\tilde{x}_{t_i}^c, t_i)$  for the corrected  $\tilde{x}_{t_i}^c$ . Although the error caused by the misalignment between  $\epsilon_\theta(\tilde{x}_{t_i}, t_i)$  and  $\epsilon_\theta(\tilde{x}_{t_i}^c, t_i)$  has no influence on the order of accuracy (as proved in Appendix E.7), we are still interested in how this error will affect the performance. Therefore, we conduct experiments where we re-compute the  $\epsilon_\theta(\tilde{x}_{t_i}^c, t_i)$  as the input for the next sampling step, which we name as “UniC-oracle”. Due to the multiple function evaluations on each  $t_i$  for both  $\tilde{x}_{t_i}$  and  $\tilde{x}_{t_i}^c$ , the real NFE for UniC-oracle is twice as the standard UniC for the same sampling steps. However, UniC-oracle is very helpful to explore the upper bound of UniC, and

**Table 4. Customizing order schedule via UniPC.** We explore the performance of UniPC of different order schedules on CIFAR10 (Krizhevsky et al., 2009). We find that some customized order schedules can yield better results than the default settings, while simply increasing the order as much as possible is harmful to the sampling quality.

CIFAR10, NFE = 6				
Order Schedule	123321	123432	123443	123456
FID↓	10.33	<b>9.03</b>	11.23	22.98
CIFAR10, NFE = 7				
Order Schedule	1233321	1223334	1234321	1234567
FID↓	6.41	<b>6.29</b>	7.24	60.99

thus can be used in pre-experiments to examine whether the corrector is potentially effective. We compare the performance of UniC and UniC-oracle in Table 3, where we apply them to the DPM Solver++ (Lu et al., 2022b) on LSUN Bedroom (Yu et al., 2015) and FFHQ (Karras et al., 2019) datasets. We observe that the UniC-oracle can significantly improve the sampling quality over the baseline methods. Although the approximation error caused by the misalignment makes UniC worse than UniC-oracle, we find that UniC can still remarkably increase the sampling quality over the baselines, especially with few sampling steps. These results also reveal that there is still room for improvement for UniC, and designing a better estimation for  $\epsilon_\theta(\tilde{x}_{t_i}^c, t_i)$  based on  $\epsilon_\theta(\tilde{x}_{t_i}, t_i)$  and history information without extra model evaluations can be an interesting direction in the future.

**Customizing order schedule via UniPC.** Thanks to the unified analytical form of UniPC, we are able to investigate the performance of arbitrary-order solvers and customize the order schedule freely. As a first attempt, we conduct experiments on CIFAR10 with our UniPC, varying the order schedule (the order at each sampling step). Some results are listed in Table 4, where we test different order schedules with NFE=6/7 because the search space is not too big. Note that the order schedule in Table 4 represents the order of accuracy of the UniP, while the actual order is increased by 1 because of UniC. Our default order schedule follows the implementation of DPM-Solver++ (Lu et al., 2022b), where lower-order solvers are used in the final few steps. Interestingly, we find some customized order schedules can yield better results, such as 123432 for NFE=6 and 1223334 for NFE=7. We also show that simply increasing the order as much as possible is harmful to the sampling quality. These findings also motivate us to investigate how to design a better order schedule, which can be potentially useful to further improve the performance of our UniPC.

**Comparisons with more NFE.** To further evaluate the effectiveness of our UniPC, we also perform experiments with 10~25 NFE. Specifically, we perform guided sampling on ImageNet 256×256 (Deng et al., 2009) with guidance scale 8.0 and compare our UniPC with more existing methods

**Table 5. Comparisons with more NFE.** We compare the sampling quality between UniPC and previous methods with 10-25 NFE on ImageNet 256×256 and show our UniPC still outperforms previous methods by a large margin.

Sampling Method \ NFE	10	15	20	25
DDIM (Song et al.)	13.04	11.27	10.21	9.87
DPM-Solver (Lu et al.)	114.62	44.05	20.33	9.84
PNDM (Liu et al.)	99.80	37.59	15.50	11.54
DEIS (Zhang & Chen)	19.12	11.37	10.08	9.75
DPM-Solver++ (Lu et al.)	9.56	8.64	8.50	8.39
UniPC (Ours)	<b>7.51</b>	<b>6.76</b>	<b>6.65</b>	<b>6.58</b>

including DDIM, DPM-Solver, PNDM, DEIS, and DPM-Solver++. We summarize the results in Table 5, where some results of the previous methods are from (Lu et al., 2022b). The results clearly demonstrate that our UniPC surpasses previous methods by a large margin.

**Visualizations.** We provide a qualitative comparison between our UniPC and previous methods with only 7 NFE, as shown in Figure 2. We use different methods to perform guided sampling with guidance scale  $s = 8.0$  from a DPM trained on ImageNet 256×256. We find that DEIS (Zhang & Chen, 2022) tends to crash with extremely few steps, while the sample generated by DDIM (Song et al., 2021a) is relatively blurry. Compared with DPM-Solver++, the state-of-the-art method in guided sampling, our method can generate more plausible samples with more visual details. We also provide more qualitative results in Appendix G.

**Limitations and broader impact.** Despite the effectiveness of UniPC, it still lags behind training-based methods such as (Salimans & Ho, 2022). How to further close the gap between training-free methods and training-based methods requires future efforts. Besides, like other methods designed for generative models, the abuse of UniPC may accelerate the generation of malicious content.

## 5. Conclusions

In this paper, we have proposed a new unified predictor-corrector framework named UniPC for the fast sampling of DPMs. Unlike previous methods, UniPC has a unified formulation for its two components (UniP and UniC) for any order. The universality of UniPC makes it possible to customize arbitrary order schedules and to improve the order of accuracy of off-the-shelf fast sampler via UniC. Extensive experiments have demonstrated the effectiveness of UniPC on unconditional/conditional sampling tasks with pixel-space/latent-space pre-trained DPMs. We have also discovered several directions where UniPC can be further improved, such as choosing a better  $B(h)$ , estimating a more accurate  $\epsilon_\theta(\tilde{x}_{t_i}^c, t_i)$ , and designing a better order schedule. We hope our attempt can inspire future work to further explore the fast sampling of DPMs in very few steps.

## References

Bao, F., Li, C., Sun, J., Zhu, J., and Zhang, B. Estimating the optimal covariance with imperfect mean in diffusion probabilistic models. *ICML*, 2022a.

Bao, F., Li, C., Zhu, J., and Zhang, B. Analytic-dpm: an analytic estimate of the optimal reverse variance in diffusion probabilistic models. *ICLR*, 2022b.

Calvo, M. P. and Palencia, C. A class of explicit multistep exponential integrators for semilinear problems. *Numerische Mathematik*, 102(3):367–381, 2006.

Chen, N., Zhang, Y., Zen, H., Weiss, R. J., Norouzi, M., and Chan, W. Wavegrad: Estimating gradients for waveform generation. *ICLR*, 2021.

Deng, J., Dong, W., Socher, R., Li, L.-J., Li, K., and Fei-Fei, L. Imagenet: A large-scale hierarchical image database. In *CVPR*, pp. 248–255. IEEE, 2009.

Dhariwal, P. and Nichol, A. Diffusion models beat gans on image synthesis. *NeurIPS*, 34:8780–8794, 2021.

Dockhorn, T., Vahdat, A., and Kreis, K. Score-based generative modeling with critically-damped langevin diffusion. *ICLR*, 2022.

Goodfellow, I., Pouget-Abadie, J., Mirza, M., Xu, B., Warde-Farley, D., Ozair, S., Courville, A., and Bengio, Y. Generative adversarial nets. In *NeurIPS*, pp. 2672–2680, 2014.

Griffiths, D. F. and Higham, D. J. *Numerical methods for ordinary differential equations: initial value problems*, volume 5. Springer, 2010.

Gu, S., Chen, D., Bao, J., Wen, F., Zhang, B., Chen, D., Yuan, L., and Guo, B. Vector quantized diffusion model for text-to-image synthesis. In *CVPR*, pp. 10696–10706, 2022.

Ho, J. and Salimans, T. Classifier-free diffusion guidance. *NeurIPS*, 2021.

Ho, J., Jain, A., and Abbeel, P. Denoising diffusion probabilistic models. *NeurIPS*, 33:6840–6851, 2020.

Ho, J., Salimans, T., Gritsenko, A., Chan, W., Norouzi, M., and Fleet, D. J. Video diffusion models. *arXiv preprint arXiv:2204.03458*, 2022.

Hochbruck, M. and Ostermann, A. Explicit exponential runge–kutta methods for semilinear parabolic problems. *SIAM Journal on Numerical Analysis*, 43(3):1069–1090, 2005.

Hochbruck, M. and Ostermann, A. Exponential integrators. *Acta Numerica*, 19:209–286, 2010. doi: 10.1017/S0962492910000048.

Karras, T., Laine, S., and Aila, T. A style-based generator architecture for generative adversarial networks. In *CVPR*, pp. 4401–4410, 2019.

Kingma, D., Salimans, T., Poole, B., and Ho, J. Variational diffusion models. *NeurIPS*, 34:21696–21707, 2021.

Kingma, D. P. and Welling, M. Auto-encoding variational bayes. *ICLR*, 2014.

Krizhevsky, A., Hinton, G., et al. Learning multiple layers of features from tiny images. 2009.

Lambert, J. D. et al. *Numerical methods for ordinary differential systems*, volume 146. Wiley New York, 1991.

Lin, T.-Y., Maire, M., Belongie, S., Hays, J., Perona, P., Ramanan, D., Dollár, P., and Zitnick, C. L. Microsoft coco: Common objects in context. In *ECCV*, pp. 740–755. Springer, 2014.

Liu, L., Ren, Y., Lin, Z., and Zhao, Z. Pseudo numerical methods for diffusion models on manifolds. *ICLR*, 2022.

Lu, C., Zhou, Y., Bao, F., Chen, J., Li, C., and Zhu, J. Dpm-solver: A fast ode solver for diffusion probabilistic model sampling in around 10 steps. *NeurIPS*, 2022a.

Lu, C., Zhou, Y., Bao, F., Chen, J., Li, C., and Zhu, J. Dpm-solver++: Fast solver for guided sampling of diffusion probabilistic models. *arXiv preprint arXiv:2211.01095*, 2022b.

Nichol, A., Dhariwal, P., Ramesh, A., Shyam, P., Mishkin, P., McGrew, B., Sutskever, I., and Chen, M. Glide: Towards photorealistic image generation and editing with text-guided diffusion models. *ICML*, 2022.

Nichol, A. Q. and Dhariwal, P. Improved denoising diffusion probabilistic models. In *ICML*, pp. 8162–8171. PMLR, 2021.

Rombach, R., Blattmann, A., Lorenz, D., Esser, P., and Ommer, B. High-resolution image synthesis with latent diffusion models. In *CVPR*, pp. 10684–10695, 2022.

Saharia, C., Chan, W., Saxena, S., Li, L., Whang, J., Denton, E., Ghasemipour, S. K. S., Ayan, B. K., Mahdavi, S. S., Lopes, R. G., et al. Photorealistic text-to-image diffusion models with deep language understanding. *NeurIPS*, 2022.

Salimans, T. and Ho, J. Progressive distillation for fast sampling of diffusion models. *ICLR*, 2022.

Schuhmann, C., Vencu, R., Beaumont, R., Kaczmarczyk, R., Mullis, C., Katta, A., Coombes, T., Jitsev, J., and Komatsuzaki, A. Laion-400m: Open dataset of clip-filtered 400 million image-text pairs. *arXiv preprint arXiv:2111.02114*, 2021.

Sohl-Dickstein, J., Weiss, E., Maheswaranathan, N., and Ganguli, S. Deep unsupervised learning using nonequilibrium thermodynamics. In *ICML*, pp. 2256–2265. PMLR, 2015.

Song, J., Meng, C., and Ermon, S. Denoising diffusion implicit models. *ICLR*, 2021a.

Song, Y., Sohl-Dickstein, J., Kingma, D. P., Kumar, A., Ermon, S., and Poole, B. Score-based generative modeling through stochastic differential equations. In *ICLR*, 2021b.

Wang, Z., Zheng, H., He, P., Chen, W., and Zhou, M. Diffusion-gan: Training gans with diffusion. *arXiv preprint arXiv:2206.02262*, 2022.

Watson, D., Chan, W., Ho, J., and Norouzi, M. Learning fast samplers for diffusion models by differentiating through sample quality. In *ICLR*, 2021.

Xiao, Z., Kreis, K., and Vahdat, A. Tackling the generative learning trilemma with denoising diffusion gans. *ICLR*, 2022.

Yu, F., Seff, A., Zhang, Y., Song, S., Funkhouser, T., and Xiao, J. Lsun: Construction of a large-scale image dataset using deep learning with humans in the loop. *arXiv preprint arXiv:1506.03365*, 2015.

Zhang, Q. and Chen, Y. Fast sampling of diffusion models with exponential integrator. *arXiv preprint arXiv:2204.13902*, 2022.

Zhang, Q., Tao, M., and Chen, Y. gddim: Generalized denoising diffusion implicit models. *arXiv preprint arXiv:2206.05564*, 2022.

## A. UniPC for Data Prediction Model

### A.1. Comparison of data prediction and noise prediction

The data prediction model is a simple linear transformation of the noise prediction model, namely  $\mathbf{x}_\theta = (\mathbf{x}_t - \sigma_t \epsilon_\theta) / \alpha_t$  (Kingma et al., 2021). However, high-order solvers based on  $\mathbf{x}_\theta$  and  $\epsilon_\theta$  are essentially different (Saharia et al., 2022; Lu et al., 2022b). As we shall see, the formulae of UniPC for the data prediction model differ from those for the noise prediction model. On the other hand, for image data,  $\mathbf{x}_\theta$  is bounded in  $[-1, 1]$ , while  $\epsilon_\theta$  is generally unbounded and thus can push the sample out of the bound. Therefore, solvers for data prediction models are preferred, since thresholding method (Saharia et al., 2022) can be directly applied and alleviate the “train-test mismatch” problem.

### A.2. Adapting UniPC to Data Prediction Model

As shown in the Proposition 4.1 of (Lu et al., 2022b), for an initial value  $\mathbf{x}_s$  at time  $s > 0$ , the solution at time  $t \in [0, s]$  of diffusion ODEs is

$$\mathbf{x}_t = \frac{\sigma_t}{\sigma_s} \mathbf{x}_s + \sigma_t \int_{\lambda_s}^{\lambda_t} e^\lambda \hat{\mathbf{x}}_\theta(\hat{\mathbf{x}}_\lambda, \lambda) d\lambda, \quad (7)$$

where we use the notation  $\hat{\mathbf{x}}_\theta$  and  $\hat{\mathbf{x}}_\lambda$  to denote changing from the domain of time ( $t$ ) to the domain of half log-SNR( $\lambda$ ), *i.e.*,  $\hat{\mathbf{x}}_\lambda := \mathbf{x}_{t_\lambda(\lambda)}$  and  $\hat{\mathbf{x}}_\theta(\cdot, \lambda) := \mathbf{x}_\theta(\cdot, t_\lambda(\lambda))$ . We are also able to adapt our UniPC to the data prediction model and utilize more information from previous data points. Recall that  $h_i = \lambda_{t_i} - \lambda_{t_{i-1}}$ . For any nonzero increasing sequence  $r_1 < r_2 < \dots < r_p = 1$ ,  $\lambda_{s_m} = r_m h_i + \lambda_{t_{i-1}}$ ,  $s_m = t_\lambda(\lambda_{s_m})$ ,  $m = 1, \dots, p$ . The UniPC- $p$  is given by

$$\tilde{\mathbf{x}}_{t_i} = \frac{\sigma_{t_i}}{\sigma_{t_{i-1}}} \tilde{\mathbf{x}}_{t_{i-1}} + \alpha_{t_i} (1 - e^{-h_i}) \mathbf{x}_\theta(\tilde{\mathbf{x}}_{t_{i-1}}, t_{i-1}) + \alpha_{t_i} B(h_i) \sum_{m=1}^{p-1} \frac{a_m}{r_m} D_m^x, \quad (\text{Predictor}) \quad (8)$$

$$\tilde{\mathbf{x}}_{t_i}^c = \frac{\sigma_{t_i}}{\sigma_{t_{i-1}}} \tilde{\mathbf{x}}_{t_{i-1}} + \alpha_{t_i} (1 - e^{-h_i}) \mathbf{x}_\theta(\tilde{\mathbf{x}}_{t_{i-1}}, t_{i-1}) + \alpha_{t_i} B(h_i) \sum_{m=1}^p \frac{c_m}{r_m} D_m^x, \quad (\text{Corrector}) \quad (9)$$

where  $D_m^x = \mathbf{x}_\theta(\tilde{\mathbf{x}}_{s_m}, s_m) - \mathbf{x}_\theta(\tilde{\mathbf{x}}_{t_{i-1}}, t_{i-1})$ . Importantly, the corrector (UniC) can be also applied to any solver for the data prediction model that outputs  $\tilde{\mathbf{x}}_{t_i}$ . Denote  $\mathbf{a}_p = (a_1, \dots, a_{p-1})^\top$ ,  $\mathbf{c}_p = (c_1, \dots, c_p)^\top$ . Let

$$\mathbf{g}_p(h) = (g_1(h), \dots, g_p(h))^\top, \quad g_n(h) = h^n n! \psi_{n+1}(h), \quad (10)$$

where  $\psi_n(h)$  is defined by the recursive relation  $\psi_{n+1}(h) = \frac{1/n! - \psi_n(h)}{h}$ ,  $\psi_0(h) = e^{-h}$ , see Appendix E.4 for details. The order of accuracy of UniPC- $p$  for the data prediction model is given by the following proposition. The proof is in Appendix E.4.

**Proposition A.1** (Order of Accuracy of UniPC- $p$  for Data Prediction Model). *For an increasing sequence  $r_1 < r_2 < \dots < r_p = 1$ , under regularity assumption E.3, assuming  $0 \neq B(h) = \mathcal{O}(h)$ ,*

$$|\mathbf{R}_p(h_i) \mathbf{c}_p B(h_i) - \mathbf{g}_p(h_i)| = \mathcal{O}(h_i^{p+1}), \text{ and } |\mathbf{R}_{p-1}(h_i) \mathbf{a}_{p-1} B(h_i) - \mathbf{g}_{p-1}(h_i)| = \mathcal{O}(h_i^p), \quad (11)$$

then the order of accuracy of UniPC- $p$  is  $p + 1$ .

We list the algorithms for UniC- $p$  and UniP- $p$  for the data prediction model separately, see Algorithm 3 and Algorithm 4.

## B. Detailed Algorithms of Multistep UniPC

This section offers detailed algorithms with warming-up for multistep UniPC for noise prediction model (Algorithm 5,Algorithm 6) and for data prediction model (Algorithm 7,Algorithm 8).

## C. UniPC with varying coefficients (UniPC<sub>v</sub>)

UniPC- $p$  (3) uses a vector  $\mathbf{a}_p$  to match simultaneously all the coefficients of the derivatives. Alternatively, we can use  $\{\mathbf{a}_{i,p}\}_{i=1}^p$  to match each order of derivatives separately and obtain a matrix of coefficients, *i.e.*,  $\mathbf{A}_p = (\mathbf{a}_{1,p}, \dots, \mathbf{a}_{p,p})^\top$ .

**Algorithm 3** UniC- $p$  for data prediction model

---

**Require:**  $\{r_i\}_{i=1}^{p-1}$ , data prediction model  $\mathbf{x}_\theta$ , any  $p$ -order solver  $\text{Solver-}p$ , an estimate at  $t_{i-1}$  namely  $\tilde{\mathbf{x}}_{t_{i-1}}$ , and a buffer  $Q$  containing previous outputs of  $\mathbf{x}_\theta$ .

$h_i \leftarrow \lambda_{t_i} - \lambda_{t_{i-1}}$ ,  $r_p \leftarrow 1$ ,  $\tilde{\mathbf{x}}_{t_i} \leftarrow \text{Solver-}p(\tilde{\mathbf{x}}_{t_{i-1}}, Q)$

**for**  $m = 1$  **to**  $p-1$  **do**

$s_m \leftarrow t_\lambda(r_m h_i + \lambda_{t_{i-1}})$

$D_m^x \leftarrow \mathbf{x}_\theta(\tilde{\mathbf{x}}_{s_m}, s_m) - \mathbf{x}_\theta(\tilde{\mathbf{x}}_{t_{i-1}}, t_{i-1})$

**end for**

Compute  $\mathbf{c}_p \leftarrow \mathbf{R}_p^{-1}(h_i) \mathbf{g}_p(h_i) / B(h_i)$ , where  $\mathbf{R}_p$  and  $\mathbf{g}_p$  are as defined in Theorem 3.1 and (10)

$\tilde{\mathbf{x}}_{t_i}^c \leftarrow \frac{\sigma_{t_i}}{\sigma_{t_{i-1}}} \tilde{\mathbf{x}}_{t_{i-1}} + \alpha_{t_i} (1 - e^{-h_i}) \mathbf{x}_\theta(\tilde{\mathbf{x}}_{t_{i-1}}, t_{i-1}) + \alpha_{t_i} B(h_i) \sum_{m=1}^p c_m D_m^x / r_m$

$Q \xleftarrow{\text{buffer}} \mathbf{x}_\theta(\tilde{\mathbf{x}}_{t_i}, t_i)$

**return:**  $\tilde{\mathbf{x}}_{t_i}^c$

---

**Algorithm 4** UniP- $p$  for the data prediction model

---

**Require:**  $\{r_i\}_{i=1}^{p-1}$ , data prediction model  $\mathbf{x}_\theta$ , an estimate at  $t_{i-1}$  namely  $\tilde{\mathbf{x}}_{t_{i-1}}$ , and a buffer  $Q$  containing previous outputs of  $\mathbf{x}_\theta$ .

$h_i \leftarrow \lambda_{t_i} - \lambda_{t_{i-1}}$

**for**  $m = 1$  **to**  $p-1$  **do**

$s_m \leftarrow t_\lambda(r_m h_i + \lambda_{t_{i-1}})$

$D_m^x \leftarrow \mathbf{x}_\theta(\tilde{\mathbf{x}}_{s_m}, s_m) - \mathbf{x}_\theta(\tilde{\mathbf{x}}_{t_{i-1}}, t_{i-1})$

**end for**

Compute  $\mathbf{a}_{p-1} \leftarrow \mathbf{R}_{p-1}^{-1}(h_i) \mathbf{g}_{p-1}(h_i) / B(h_i)$ , where  $\mathbf{R}_{p-1}$  and  $\mathbf{g}_{p-1}$  are as defined in Theorem 3.1 and (10)

$\tilde{\mathbf{x}}_{t_i} \leftarrow \frac{\sigma_{t_i}}{\sigma_{t_{i-1}}} \tilde{\mathbf{x}}_{t_{i-1}} + \alpha_{t_i} (1 - e^{-h_i}) \mathbf{x}_\theta(\tilde{\mathbf{x}}_{t_{i-1}}, t_{i-1}) + \alpha_{t_i} B(h_i) \sum_{m=1}^{p-1} a_m D_m^x / r_m$

$Q \xleftarrow{\text{buffer}} \mathbf{x}_\theta(\tilde{\mathbf{x}}_{t_i}, t_i)$

**return:**  $\tilde{\mathbf{x}}_{t_i}$

---

Consider

$$\tilde{\mathbf{x}}_{t_i} = \frac{\alpha_{t_i}}{\alpha_{t_{i-1}}} \tilde{\mathbf{x}}_{t_{i-1}} - \sigma_{t_i} (e^{h_i} - 1) \epsilon_\theta(\tilde{\mathbf{x}}_{t_{i-1}}, t_{i-1}) - \sigma_{t_i} \sum_{n=1}^p h_i \varphi_{n+1}(h_i) \mathbf{a}_{n,p}^\top \mathbf{D}_p, \quad (12)$$

where  $\mathbf{D}_p = (D_1/r_1, \dots, D_p/r_p)^\top$  and  $D_m$  is defined in (4). The following theorem guarantees the order of accuracy of UniPC<sub>v</sub>. The proof is deferred to Appendix E. The convergence order is investigated in Appendix D. Define

$$\mathbf{C}_p = \begin{pmatrix} 1 & 1 & \cdots & 1 \\ r_1/2! & r_2/2! & \cdots & r_p/2! \\ \vdots & \vdots & \ddots & \vdots \\ r_1^{p-1}/p! & r_2^{p-1}/p! & \cdots & r_p^{p-1}/p! \end{pmatrix}.$$

Let  $\mathbf{I}_p$  be the  $p$ -dimensional identity matrix.

**Theorem C.1.** *Under the conditions of Theorem 3.1, if*

$$|\mathbf{C}_p \mathbf{A}_p - \mathbf{I}_p| = \mathcal{O}(h^p), \quad h = \max_{1 \leq i \leq p} h_i, \quad (13)$$

UniPC<sub>v</sub> is  $(p+1)$ -th order accurate.

In fact,  $\mathbf{C}_p$  is invertible. Note that  $\mathbf{C}_p$  is the product of a diagonal matrix and a Vandermonde matrix, namely

$$\mathbf{C}_p = \begin{pmatrix} 1 & & & \\ & \ddots & & \\ & & 1/p! \end{pmatrix} \begin{pmatrix} 1 & 1 & \cdots & 1 \\ r_1 & r_2 & \cdots & r_p \\ \vdots & \vdots & \ddots & \vdots \\ r_1^{p-1} & r_2^{p-1} & \cdots & r_p^{p-1} \end{pmatrix}, \quad r_1 < \cdots < r_p.$$

**Algorithm 5** Detailed implementation of multistep UniC- $p$ 


---

**Require:** initial value  $\mathbf{x}_T$ , time steps  $\{t_i\}_{i=0}^M$ , noise prediction model  $\epsilon_\theta$ , any  $p$ -order solver  $\text{Solver-}p$   
Denote  $h_i := \lambda_{t_i} - \lambda_{t_{i-1}}$ , for  $i = 1, \dots, M$ .  
 $\tilde{\mathbf{x}}_{t_0} \leftarrow \mathbf{x}_T$ . Initialize an empty buffer  $Q$ .  
 $Q \xleftarrow{\text{buffer}} \epsilon_\theta(\tilde{\mathbf{x}}_{t_0}, t_0)$   
**for**  $i = 1$  **to**  $M$  **do**  
 $p_i \leftarrow \min\{p, i\}$   
 $\tilde{\mathbf{x}}_{t_i}^{(1)} \leftarrow \frac{\alpha_{t_i}}{\alpha_{t_{i-1}}} \tilde{\mathbf{x}}_{t_{i-1}}^c - \sigma_{t_i} (e^{h_i} - 1) \epsilon_\theta(\tilde{\mathbf{x}}_{t_{i-1}}, t_{i-1})$   
 $\tilde{\mathbf{x}}_{t_i} \leftarrow \text{Solver-}p_i(\tilde{\mathbf{x}}_{t_{i-1}}^c, Q)$   
 $r_{p_i} \leftarrow 1$   
 $D_{p_i} \leftarrow \epsilon_\theta(\tilde{\mathbf{x}}_{t_i}, t_i) - \epsilon_\theta(\tilde{\mathbf{x}}_{t_{i-1}}, t_{i-1})$   
**for**  $m = 2$  **to**  $p_i$  **do**  
 $r_{m-1} \leftarrow (\lambda_{t_{i-m}} - \lambda_{t_{i-1}})/h_i$   
 $D_{m-1} \leftarrow \epsilon_\theta(\tilde{\mathbf{x}}_{t_{i-m}}, t_{i-m}) - \epsilon_\theta(\tilde{\mathbf{x}}_{t_{i-1}}, t_{i-1})$   
**end for**  
Compute  $\mathbf{a}_{p_i} \leftarrow \mathbf{R}_{p_i}^{-1}(h_i) \phi_{p_i}(h_i) / B(h_i)$ , where  $\mathbf{R}_{p_i}^{-1}(h_i)$  and  $\phi_{p_i}$  are as defined in Theorem 3.1.  
 $\tilde{\mathbf{x}}_{t_i}^c \leftarrow \tilde{\mathbf{x}}_{t_i}^{(1)} - \sigma_{t_i} B(h_i) \sum_{m=1}^{p_i} a_m D_m / r_m$   
 $Q \xleftarrow{\text{buffer}} \epsilon_\theta(\tilde{\mathbf{x}}_{t_i}, t_i)$   
**end for**  
**return:**  $\tilde{\mathbf{x}}_{t_M}$ 


---

Thus, we can simply take  $\mathbf{A}_p = \mathbf{C}_p^{-1}$ . The advantage of UniPC<sub>v</sub> is that  $\mathbf{A}_p$  solely depends on  $\{r_i\}_{i=1}^p$ . The algorithm of UniPC<sub>v</sub> is to replace the updating formulae of UniPC (Algorithm 1 and Algorithm 2) by (12) with  $\mathbf{A}_p = \mathbf{C}_p^{-1}$ . See Appendix G for its performance.

## D. Order of Convergence

In this section, we shall show that under mild conditions the convergence order of UniP- $p$  is  $p$  and the convergence order of UniPC- $p$  is  $p+1$  for either the noise prediction model or data prediction model. The proof is deferred to Appendix E.

**Definition D.1.** For time steps  $\{t_i\}_{i=0}^M$ , we say the order of convergence of a sampler for DPMs is  $p$  if

$$|\tilde{\mathbf{x}}_{t_M} - \mathbf{x}_0| = \mathcal{O}(h^p).$$

We start by introducing some additional regularity assumptions.

**Assumption D.2.** The noise prediction model  $\epsilon_\theta(\mathbf{x}, s)$  is Lipschitz continuous w.r.t.  $\mathbf{x}$  with Lipschitz constant  $L$ .

**Assumption D.3.** (1)  $h = \max_{1 \leq i \leq M} h_i = \mathcal{O}(1/M)$  (2) For a constant  $b > 0$ ,  $\max_{1 \leq i \leq M} L\alpha_{t_{i-1}}/\alpha_{t_i} < b$ ,  $b^{-1} < \alpha_{t_i} < b$ , for all  $1 \leq i \leq M$ .

**Assumption D.4.** The starting values  $\tilde{\mathbf{x}}_{t_i}$ ,  $1 \leq i \leq k-1$  satisfies for some positive constant  $c_0$ ,

$$|\mathbf{x}_{t_i} - \tilde{\mathbf{x}}_{t_i}| \leq c_0 h^k, \quad 1 \leq i \leq k-1. \quad (14)$$

Assumption D.2 is common in the analysis of ODEs similar to (18). By Assumption D.2, we have  $\epsilon_\theta(\tilde{\mathbf{x}}_s, s) = \epsilon_\theta(\mathbf{x}_s, s) + \mathcal{O}(\tilde{\mathbf{x}}_s - \mathbf{x}_s)$ . Assumption D.3 assures that there is no significantly large step size and the signals are neither exploding nor degenerating. Assumption D.4 is common in the convergence analysis of multistep approaches (Calvo & Palencia, 2006).

The following Propositions D.5 and D.6 ensure the convergence order of UniP- $p$  and UniPC- $p$ . For general  $\text{Solver-}p$  such as DDIM ( $p=1$ ), DPM-Solver/DPM-Solver++ ( $p \leq 3$ ), UniC- $p$  can also increase the convergence order.

**Proposition D.5.** *Under the conditions of Theorem 3.1, Assumptions D.2, D.3, and D.4, the order of convergence of UniP- $p$  is  $p$ .*

**Proposition D.6.** *Under the conditions of Theorem 3.1, Assumptions D.2, D.3, and D.4 with  $k=p$ , the order of convergence of UniPC- $p$  is  $p+1$ .*

**Algorithm 6** Detailed implementation of multistep UniP- $p$ 


---

**Require:** initial value  $\mathbf{x}_T$ , time steps  $\{t_i\}_{i=0}^M$ , noise prediction model  $\epsilon_\theta$   
Denote  $h_i := \lambda_{t_i} - \lambda_{t_{i-1}}$ , for  $i = 1, \dots, M$ .  
 $\tilde{\mathbf{x}}_{t_0} \leftarrow \mathbf{x}_T$ . Initialize an empty buffer  $Q$ .  
 $Q \xleftarrow{\text{buffer}} \epsilon_\theta(\tilde{\mathbf{x}}_{t_0}, t_0)$   
**for**  $i = 1$  **to**  $M$  **do**  
     $p_i \leftarrow \min\{p, i\}$   
     $\tilde{\mathbf{x}}_{t_i}^{(1)} \leftarrow \frac{\alpha_{t_i}}{\alpha_{t_{i-1}}} \tilde{\mathbf{x}}_{t_{i-1}} - \sigma_{t_i} (e^{h_i} - 1) \epsilon_\theta(\tilde{\mathbf{x}}_{t_{i-1}}, t_{i-1})$   
    **if**  $p_i = 1$  **then**  
         $\tilde{\mathbf{x}}_{t_i} \leftarrow \tilde{\mathbf{x}}_{t_i}^{(1)}$   
         $Q \xleftarrow{\text{buffer}} \epsilon_\theta(\tilde{\mathbf{x}}_{t_i}, t_i)$   
        **continue**  
    **end if**  
    **for**  $m = 2$  **to**  $p_i$  **do**  
         $r_{m-1} \leftarrow (\lambda_{t_{i-m}} - \lambda_{t_{i-1}})/h_i$   
         $D_{m-1} \leftarrow \epsilon_\theta(\tilde{\mathbf{x}}_{t_{i-m}}, t_{i-m}) - \epsilon_\theta(\tilde{\mathbf{x}}_{t_{i-1}}, t_{i-1})$   
    **end for**  
    Compute  $\mathbf{a}_{p_i-1} \leftarrow \mathbf{R}_{p_i-1}^{-1}(h_i) \phi_{p_i-1}(h_i) / B(h_i)$ , where  $\mathbf{R}_{p_i-1}^{-1}(h_i)$  and  $\phi_{p_i-1}$  are as defined in Theorem 3.1.  
     $\tilde{\mathbf{x}}_{t_i} \leftarrow \tilde{\mathbf{x}}_{t_i}^{(1)} - \sigma_{t_i} B(h_i) \sum_{m=1}^{p_i-1} a_m D_m / r_m$   
     $Q \xleftarrow{\text{buffer}} \epsilon_\theta(\tilde{\mathbf{x}}_{t_i}, t_i)$   
**end for**  
**return:**  $\tilde{\mathbf{x}}_{t_M}$ 


---

*Remark D.7.* After a careful investigation of the proof of Proposition D.6 and Proposition D.5, we point out that for the singlestep updating when using UniPC-1 for the estimation of  $\tilde{\mathbf{x}}_{s_m}$ ,  $t_{i-1} < s_1, \dots, s_m < t_i$ , the order of convergence for UniPC- $p$  is  $p + 1$  and the order of convergence for UniP- $p$  is  $p$  for  $p \leq 3$ .

Following similar arguments of Proposition D.6, we find that UniC- $p$  can also increase the convergence order for general Solver- $p$  for diffusion ODEs. The following is a direct corollary of Proposition D.6 which gives the order of convergence of UniPC<sub>v</sub>- $p$ .

**Corollary D.8.** *Under the conditions of Theorem C.1, Assumptions D.2, D.3, and D.4 with  $k = p$ , the order of convergence of UniPC<sub>v</sub>- $p$  is  $p + 1$ .*

The order of convergence for the data prediction model follows analogous to Proposition D.5 and Proposition D.6 under slightly different assumptions:

**Assumption D.9.** The noise prediction model  $\mathbf{x}_\theta(\mathbf{x}, s)$  is Lipschitz continuous w.r.t.  $\mathbf{x}$  with Lipschitz constant  $L$ .

**Assumption D.10.** (1)  $h = \max_{1 \leq i \leq M} h_i = \mathcal{O}(1/M)$  (2) For a constant  $b > 0$ ,  $\max_{1 \leq i \leq M} L\sigma_{t_{i-1}}/\sigma_{t_i} < b$ ,  $b^{-1} < \sigma_{t_i} < b$ , for all  $1 \leq i \leq M$ .

We list the results of the order of convergence of UniP and UniPC for the data prediction model as corollaries to Propositions D.5 and D.6 and omit their proofs for simplicity. Interested readers can refer to the arguments in Appendix E for the noise prediction model and derive the detailed proofs for the data prediction model.

**Corollary D.11.** *Under the conditions of Proposition A.1, Assumptions D.9, D.10, and D.4 with  $k = p$ , the order of convergence of UniP- $p$  for data prediction model is  $p$ .*

**Corollary D.12.** *Under the conditions of Proposition A.1, Assumptions D.9, D.10, and D.4 with  $k = p$ , the order of convergence of UniPC- $p$  for data prediction model is  $p + 1$ .*

## E. Proofs

In this section, we provide preliminaries of numerical analysis, regularity assumption, and the proof of Theorem 3.1 in the paper, the regularity assumption and the proof of Proposition A.1 in Appendix A as well as detailed proofs for Theorem C.1

**Algorithm 7** Detailed implementation of multistep UniC- $p$  for data prediction model

---

**Require:** initial value  $\mathbf{x}_T$ , time steps  $\{t_i\}_{i=0}^M$ , data prediction model  $\mathbf{x}_\theta$ , any p-order solver `Solver-p`  
Denote  $h_i := \lambda_{t_i} - \lambda_{t_{i-1}}$ , for  $i = 1, \dots, M$ .  
 $\tilde{\mathbf{x}}_{t_0} \leftarrow \mathbf{x}_T$ . Initialize an empty buffer  $Q$ .  
 $Q \xleftarrow{\text{buffer}} \mathbf{x}_\theta(\tilde{\mathbf{x}}_{t_0}, t_0)$   
**for**  $i = 1$  **to**  $M$  **do**  
 $p_i \leftarrow \min\{p, i\}$   
 $\tilde{\mathbf{x}}_{t_i}^{(1)} \leftarrow \frac{\sigma_{t_i}}{\sigma_{t_{i-1}}} \tilde{\mathbf{x}}_{t_{i-1}}^c + \alpha_{t_i} (1 - e^{-h_i}) \mathbf{x}_\theta(\tilde{\mathbf{x}}_{t_{i-1}}, t_{i-1})$   
 $\tilde{\mathbf{x}}_{t_i} \leftarrow \text{Solver-p}_i(\tilde{\mathbf{x}}_{t_{i-1}}^c, Q)$   
 $r_{p_i} \leftarrow 1$   
 $D_{p_i} \leftarrow \mathbf{x}_\theta(\tilde{\mathbf{x}}_{t_i}, t_i) - \mathbf{x}_\theta(\tilde{\mathbf{x}}_{t_{i-1}}, t_{i-1})$   
**for**  $m = 2$  **to**  $p_i$  **do**  
 $r_{m-1} \leftarrow (\lambda_{t_{i-m}} - \lambda_{t_{i-1}})/h_i$   
 $D_{m-1}^x \leftarrow \mathbf{x}_\theta(\tilde{\mathbf{x}}_{t_{i-m}}, t_{i-m}) - \mathbf{x}_\theta(\tilde{\mathbf{x}}_{t_{i-1}}, t_{i-1})$   
**end for**  
Compute  $c_{p_i} \leftarrow \mathbf{R}_{p_i}^{-1}(h_i) \mathbf{g}_{p_i}(h_i)/B(h_i)$ , where  $\mathbf{R}_{p_i}^{-1}(h_i)$  and  $\mathbf{g}_{p_i}$  are as defined in Theorem 3.1 and (10).  
 $\tilde{\mathbf{x}}_{t_i}^c \leftarrow \tilde{\mathbf{x}}_{t_i}^{(1)} + \alpha_{t_i} B(h_i) \sum_{m=1}^{p_i} c_m D_m^x / r_m$   
 $Q \xleftarrow{\text{buffer}} \mathbf{x}_\theta(\tilde{\mathbf{x}}_{t_i}, t_i)$   
**end for**  
**return:**  $\tilde{\mathbf{x}}_{t_M}$ 


---

in Appendix C, for Proposition D.5 and Proposition D.6 in Appendix D. Through this section, we use  $C$  and  $C_i$  to denote sufficiently large positive constants independent of  $h$ .

## E.1. Preliminaries

We begin with introducing preliminary results and concepts necessary for the proof of Theorem 3.1.

**Expansion of exponential integrator.** First, we obtain the Taylor expansion of (2), namely the exponentially weighted integral. Define the  $k$ -th order derivative of  $\hat{\epsilon}_\theta(\hat{\mathbf{x}}_\lambda, \lambda)$  as  $\hat{\epsilon}_\theta^{(k)}(\hat{\mathbf{x}}_\lambda, \lambda) := d^k \hat{\epsilon}_\theta(\hat{\mathbf{x}}_\lambda, \lambda) / d\lambda^k$ . For  $0 \leq t < s \leq T$ ,  $r \in [0, 1]$ , let  $h := \lambda_t - \lambda_s$ ,  $\lambda := \lambda_s + rh$ . Assuming the existence of total derivatives of  $\hat{\epsilon}_\theta^{(k)}(\hat{\mathbf{x}}_\lambda, \lambda)$ ,  $0 \leq k \leq n$ , we have the  $n$ -th order Taylor expansion of  $\hat{\epsilon}_\theta(\hat{\mathbf{x}}_\lambda, \lambda)$  w.r.t. the half log-SNR  $\lambda$ :

$$\hat{\epsilon}_\theta(\hat{\mathbf{x}}_\lambda, \lambda) = \sum_{k=0}^n \frac{r^k h^k}{k!} \hat{\epsilon}_\theta^{(k)}(\hat{\mathbf{x}}_{\lambda_s}, \lambda_s) + \mathcal{O}(h^{n+1}). \quad (15)$$

Using the result of Taylor expansion of (15), the exponential integrator of (2) can be reduced to

$$\begin{aligned} \int_{\lambda_s}^{\lambda_t} e^{-\lambda} \hat{\epsilon}_\theta(\hat{\mathbf{x}}_\lambda, \lambda) d\lambda &= \frac{\sigma_t}{\alpha_t} \sum_{k=0}^n h^{k+1} \int_0^1 e^{\lambda_t - \lambda} \frac{r^k}{k!} dr \hat{\epsilon}_\theta^{(k)}(\hat{\mathbf{x}}_{\lambda_s}, \lambda_s) + \mathcal{O}(h^{n+2}) \\ &= \frac{\sigma_t}{\alpha_t} \sum_{k=0}^n h^{k+1} \int_0^1 e^{(1-r)h} \frac{r^k}{k!} dr \hat{\epsilon}_\theta^{(k)}(\hat{\mathbf{x}}_{\lambda_s}, \lambda_s) + \mathcal{O}(h^{n+2}) \\ &:= \frac{\sigma_t}{\alpha_t} \sum_{k=0}^n h^{k+1} \varphi_{k+1}(h) \hat{\epsilon}_\theta^{(k)}(\hat{\mathbf{x}}_{\lambda_s}, \lambda_s) + \mathcal{O}(h^{n+2}), \end{aligned} \quad (16)$$

where  $\varphi_{k+1}(h) = \int_0^1 e^{(1-r)h} \frac{r^k}{k!} dr$  can be computed via the recurrence relation  $\varphi_{k+1}(z) = (\varphi_k(z) - \varphi_k(0))/z$ ,  $\varphi_k(0) = 1/k!$ , and  $\varphi_0(z) = e^z$  (Hochbruck & Ostermann, 2005). For example, the closed-forms of  $\varphi_k(h)$  for  $k = 1, 2, 3$  are

$$\varphi_1(h) = \frac{e^h - 1}{h}, \quad \varphi_2(h) = \frac{e^h - h - 1}{h^2}, \quad \varphi_3(h) = \frac{e^h - h^2/2 - h - 1}{h^3}.$$

**Algorithm 8** Detailed implementation of multistep UniP- $p$  for data prediction model

---

**Require:** initial value  $\mathbf{x}_T$ , time steps  $\{t_i\}_{i=0}^M$ , data prediction model  $\mathbf{x}_\theta$   
Denote  $h_i := \lambda_{t_i} - \lambda_{t_{i-1}}$ , for  $i = 1, \dots, M$ .  
 $\tilde{\mathbf{x}}_{t_0} \leftarrow \mathbf{x}_T$ . Initialize an empty buffer  $Q$ .  
 $Q \xleftarrow{\text{buffer}} \mathbf{x}_\theta(\tilde{\mathbf{x}}_{t_0}, t_0)$   
**for**  $i = 1$  **to**  $M$  **do**  
     $p_i \leftarrow \min\{p, i\}$   
     $\tilde{\mathbf{x}}_{t_i}^{(1)} \leftarrow \frac{\sigma_{t_i}}{\sigma_{t_{i-1}}} \tilde{\mathbf{x}}_{t_{i-1}} + \alpha_{t_i} (1 - e^{-h_i}) \mathbf{x}_\theta(\tilde{\mathbf{x}}_{t_{i-1}}, t_{i-1})$   
    **if**  $p_i = 1$  **then**  
         $\tilde{\mathbf{x}}_{t_i} \leftarrow \tilde{\mathbf{x}}_{t_i}^{(1)}$   
         $Q \xleftarrow{\text{buffer}} \mathbf{x}_\theta(\tilde{\mathbf{x}}_{t_i}, t_i)$   
        **continue**  
    **end if**  
    **for**  $m = 2$  **to**  $p_i$  **do**  
         $r_{m-1} \leftarrow (\lambda_{t_{i-m}} - \lambda_{t_{i-1}})/h_i$   
         $D_{m-1}^x \leftarrow \mathbf{x}_\theta(\tilde{\mathbf{x}}_{t_{i-m}}, t_{i-m}) - \mathbf{x}_\theta(\tilde{\mathbf{x}}_{t_{i-1}}, t_{i-1})$   
    **end for**  
    Compute  $\mathbf{a}_{p_i-1} \leftarrow \mathbf{R}_{p_i-1}^{-1}(h_i) \mathbf{g}_{p_i-1}(h_i)/B(h_i)$ , where  $\mathbf{R}_{p_i-1}^{-1}(h_i)$  and  $\mathbf{g}_{p_i-1}$  are as defined in Theorem 3.1 and (10).  
     $\tilde{\mathbf{x}}_{t_i} \leftarrow \tilde{\mathbf{x}}_{t_i}^{(1)} + \alpha_{t_i} B(h_i) \sum_{m=1}^{p_i-1} a_m D_m^x / r_m$   
     $Q \xleftarrow{\text{buffer}} \mathbf{x}_\theta(\tilde{\mathbf{x}}_{t_i}, t_i)$   
**end for**  
**return:**  $\tilde{\mathbf{x}}_{t_M}$ 


---

**Order of accuracy.** In the following, we use the linear multistep method to illustrate the order of accuracy. Consider the ODE

$$y' = f(x, y), x \in [x_0, b], \quad y(x_0) = y_0. \quad (17)$$

We say that  $f$  satisfies Lipschitz condition, if there exists  $L > 0$  such that

$$|f(x, y_1) - f(x, y_2)| \leq L|y_1 - y_2|, \forall y_1, y_2 \in \mathbb{R}. \quad (18)$$

Suppose  $y(x)$  is the solution of Equation (17).

The  $k$ -order linear multistep method is given by

$$y_{n+k} = \sum_{i=0}^{k-1} \alpha_i y_{n+i} + h \sum_{i=0}^k \beta_i f(x_{n+i}, y_{n+i}), \quad (19)$$

where  $y_{n+i}$  is the approximation of  $y(x_{n+i})$ ,  $x_{n+i} = x_n + ih$ ,  $\alpha_i, \beta_i$  are constants,  $|\alpha_0| + |\beta_0| > 0$ .

**Definition E.1.** The local truncation error of (19) on  $x_{n+k}$  is

$$T_{n+k} = y(x_{n+k}) - \sum_{i=0}^{k-1} \alpha_i y(x_{n+i}) - h \sum_{i=0}^k \beta_i f(x_{n+i}, y(x_{n+i})). \quad (20)$$

If  $T_{n+k} = \mathcal{O}(h^{p+1})$ , we say the order of accuracy of (19) is  $p$ .

The local truncation error describes the error caused by *one iteration* in the numerical analysis (Lambert et al., 1991).

## E.2. Regularity Assumption

**Assumption E.2.** The total derivatives  $\frac{d^k \hat{\epsilon}_\theta(\hat{\mathbf{x}}_\lambda, \lambda)}{d\lambda_k}$ ,  $k = 1, \dots, p$  exist and are continuous.

Assumption E.2 is required for the Taylor expansion which is also regular in high-order numerical methods.

**E.3. Proof of Theorem 3.1 for arbitrary  $p \geq 1$** 

We first give the local truncation error of UniC. Define

$$\bar{\mathbf{x}}_{t_i} = \frac{\alpha_{t_i}}{\alpha_{t_{i-1}}} \mathbf{x}_{t_{i-1}} - \sigma_{t_i} (e^{h_i} - 1) \boldsymbol{\epsilon}_\theta(\mathbf{x}_{t_{i-1}}, t_{i-1}) - \sigma_{t_i} B(h_i) \sum_{m=1}^{p-1} \frac{a_m}{r_m} (\hat{\boldsymbol{\epsilon}}_\theta(\hat{\mathbf{x}}_{\lambda_{s_m}}, \lambda_{s_m}) - \hat{\boldsymbol{\epsilon}}_\theta(\hat{\mathbf{x}}_{\lambda_{t_{i-1}}}, \lambda_{t_{i-1}})) - \sigma_{t_i} B(h_i) \frac{a_p}{r_p} (\boldsymbol{\epsilon}_\theta(\tilde{\mathbf{x}}_{t_i}, t_i) - \hat{\boldsymbol{\epsilon}}_\theta(\hat{\mathbf{x}}_{\lambda_{t_{i-1}}}, \lambda_{t_{i-1}})).$$

Since  $\text{Solver-p}$  has order of accuracy  $p$  and  $B(h) = \mathcal{O}(h)$ , under Assumption D.2, we have

$$\bar{\mathbf{x}}_{t_i} = \frac{\alpha_{t_i}}{\alpha_{t_{i-1}}} \mathbf{x}_{t_{i-1}} - \sigma_{t_i} (e^{h_i} - 1) \boldsymbol{\epsilon}_\theta(\mathbf{x}_{t_{i-1}}, t_{i-1}) - \sigma_{t_i} B(h_i) \sum_{m=1}^p \frac{a_m}{r_m} (\hat{\boldsymbol{\epsilon}}_\theta(\hat{\mathbf{x}}_{\lambda_{s_m}}, \lambda_{s_m}) - \hat{\boldsymbol{\epsilon}}_\theta(\hat{\mathbf{x}}_{\lambda_{t_{i-1}}}, \lambda_{t_{i-1}})) + \mathcal{O}(h^{p+2}). \quad (21)$$

Suppose  $\mathbf{x}_t$  is the solution of the diffusion ODE (1). Then, the local truncation error on  $t_i$  is given by  $|\mathbf{x}_{t_i} - \bar{\mathbf{x}}_{t_i}|$ . Further, similar to Definition E.1 the order of accuracy of UniC is  $l$ , if there exists a sufficiently large positive constant  $C$  such that

$$\max_{1 \leq i \leq M} |\mathbf{x}_{t_i} - \bar{\mathbf{x}}_{t_i}| \leq Ch^{l+1}, \quad h = \max_{1 \leq i \leq M} h_i.$$

In the following, we shall show that the order of accuracy of UniC- $p$  is  $p+1$ . Combining (2) and (15), we have

$$\begin{aligned} \mathbf{x}_{t_i} &= \frac{\alpha_{t_i}}{\alpha_{t_{i-1}}} \mathbf{x}_{t_{i-1}} - \alpha_{t_i} \int_{\lambda_{t_{i-1}}}^{\lambda_{t_i}} e^{-\lambda} \hat{\boldsymbol{\epsilon}}_\theta(\hat{\mathbf{x}}_\lambda, \lambda) d\lambda \\ &= \frac{\alpha_{t_i}}{\alpha_{t_{i-1}}} \mathbf{x}_{t_{i-1}} - \sigma_{t_i} \sum_{k=0}^p h_i^{k+1} \varphi_{k+1}(h_i) \hat{\boldsymbol{\epsilon}}_\theta^{(k)}(\hat{\mathbf{x}}_{\lambda_{t_{i-1}}}, \lambda_{t_{i-1}}) + \mathcal{O}(h^{p+2}) \\ &= \frac{\alpha_{t_i}}{\alpha_{t_{i-1}}} \mathbf{x}_{t_{i-1}} - \sigma_{t_i} (e^{h_i} - 1) \boldsymbol{\epsilon}_\theta(\mathbf{x}_{t_{i-1}}, t_{i-1}) - \sigma_{t_i} \sum_{k=1}^p h_i^{k+1} \varphi_{k+1}(h_i) \hat{\boldsymbol{\epsilon}}_\theta^{(k)}(\hat{\mathbf{x}}_{\lambda_{t_{i-1}}}, \lambda_{t_{i-1}}) + \mathcal{O}(h^{p+2}). \end{aligned} \quad (22)$$

Let  $\mathbf{R}_{p,k}^\top$  denote the  $k$ -th row of  $\mathbf{R}_p$ . By (5), we have  $|\mathbf{a}_p^\top \mathbf{R}_{p,k}(h_i) - B^{-1}(h_i) h_i^k k! \varphi_{k+1}(h_i)| \leq C_0 B^{-1}(h_i) h_i^{p+1}$ . Under Assumption E.2, by Taylor expansion, we obtain

$$\begin{aligned} &\sum_{m=1}^p \frac{a_m}{r_m} (\hat{\boldsymbol{\epsilon}}_\theta(\hat{\mathbf{x}}_{\lambda_{s_m}}, \lambda_{s_m}) - \hat{\boldsymbol{\epsilon}}_\theta(\hat{\mathbf{x}}_{\lambda_{t_{i-1}}}, \lambda_{t_{i-1}})) \\ &= \sum_{m=1}^p a_m \sum_{n=1}^p \frac{r_m^{n-1} h_i^n}{n!} \hat{\boldsymbol{\epsilon}}_\theta^{(n)}(\hat{\mathbf{x}}_{\lambda_{t_{i-1}}}, \lambda_{t_{i-1}}) + \mathcal{O}(h^{p+1}) \\ &= \sum_{n=1}^p \sum_{m=1}^p a_m \frac{r_m^{n-1} h_i^n}{n!} \hat{\boldsymbol{\epsilon}}_\theta^{(n)}(\hat{\mathbf{x}}_{\lambda_{t_{i-1}}}, \lambda_{t_{i-1}}) + \mathcal{O}(h^{p+1}) \\ &= \sum_{n=1}^p \frac{h_i}{n!} \mathbf{a}_p^\top \mathbf{R}_{p,n}(h_i) \hat{\boldsymbol{\epsilon}}_\theta^{(n)}(\hat{\mathbf{x}}_{\lambda_{t_{i-1}}}, \lambda_{t_{i-1}}) + \mathcal{O}(h^{p+1}). \end{aligned}$$

Thus, we have

$$\begin{aligned} &\left| \sum_{m=1}^p \frac{a_m}{r_m} (\hat{\boldsymbol{\epsilon}}_\theta(\hat{\mathbf{x}}_{\lambda_{s_m}}, \lambda_{s_m}) - \hat{\boldsymbol{\epsilon}}_\theta(\hat{\mathbf{x}}_{\lambda_{t_{i-1}}}, \lambda_{t_{i-1}})) - B(h_i)^{-1} \sum_{k=1}^p h_i^{k+1} \varphi_{k+1}(h_i) \hat{\boldsymbol{\epsilon}}_\theta^{(k)}(\hat{\mathbf{x}}_{\lambda_{t_{i-1}}}, \lambda_{t_{i-1}}) \right| \\ &\leq C_1 (B(h_i)^{-1} h_i^{p+2} + h^{p+1}). \end{aligned} \quad (23)$$

Combining (21), (22) and (23) given  $B(h_i) = \mathcal{O}(h_i)$ , we have

$$\begin{aligned} \max_{1 \leq i \leq M} |\mathbf{x}_{t_i} - \bar{\mathbf{x}}_{t_i}| &= \left| -\sigma_{t_i} \sum_{k=1}^p h_i^{k+1} \varphi_{k+1}(h_i) \hat{\epsilon}_\theta^{(k)}(\hat{\mathbf{x}}_{\lambda_{t_{i-1}}}, \lambda_{t_{i-1}}) \right. \\ &\quad \left. + \sigma_{t_i} B(h_i) \sum_{m=1}^p \frac{a_m}{r_m} (\hat{\epsilon}_\theta(\hat{\mathbf{x}}_{\lambda_{s_m}}, \lambda_{s_m}) - \hat{\epsilon}_\theta(\hat{\mathbf{x}}_{\lambda_{t_{i-1}}}, \lambda_{t_{i-1}})) \right| + \mathcal{O}(h^{p+2}) \\ &= \mathcal{O}(h^{p+2}). \end{aligned} \quad (24)$$

Therefore, UniC- $p$  is of  $(p+1)$ -th order of accuracy.  $\square$

#### E.4. Proof of Proposition A.1

##### Regularity Assumption

**Assumption E.3.** The total derivatives  $\frac{d^k \hat{\mathbf{x}}_\theta(\hat{\mathbf{x}}_\lambda, \lambda)}{d\lambda_k}$ ,  $k = 1, \dots, p$  exist and are continuous.

**Expansion of the Exponentially Weighted Integral.** First, we obtain the Taylor expansion of (7). Define the  $k$ -th order derivative of  $\hat{\mathbf{x}}_\theta(\hat{\mathbf{x}}_\lambda, \lambda)$  as  $\hat{\mathbf{x}}_\theta^{(k)}(\hat{\mathbf{x}}_\lambda, \lambda) := d^k \hat{\mathbf{x}}_\theta(\hat{\mathbf{x}}_\lambda, \lambda) / d\lambda^k$ . For  $0 \leq t < s \leq T$ ,  $r \in [0, 1]$ , let  $h := \lambda_t - \lambda_s$ ,  $\lambda := \lambda_s + rh$ . Assuming the existence of total derivatives of  $\hat{\mathbf{x}}_\theta^{(k)}(\hat{\mathbf{x}}_\lambda, \lambda)$ ,  $0 \leq k \leq n$ , the  $n$ -th order Taylor expansion of  $\hat{\mathbf{x}}_\theta(\hat{\mathbf{x}}_\lambda, \lambda)$  w.r.t. the half log-SNR  $\lambda$  is:

$$\hat{\mathbf{x}}_\theta(\hat{\mathbf{x}}_\lambda, \lambda) = \sum_{k=0}^n \frac{r^k h^k}{k!} \hat{\mathbf{x}}_\theta^{(k)}(\hat{\mathbf{x}}_{\lambda_s}, \lambda_s) + \mathcal{O}(h^{n+1}). \quad (25)$$

Then, the exponential integrator of (7) can be reduced to

$$\begin{aligned} \int_{\lambda_s}^{\lambda_t} e^\lambda \hat{\mathbf{x}}_\theta(\hat{\mathbf{x}}_\lambda, \lambda) d\lambda &= \frac{\alpha_t}{\sigma_t} \sum_{k=0}^n h^{k+1} \int_0^1 e^{\lambda - \lambda_t} \frac{r^k}{k!} dr \hat{\mathbf{x}}_\theta^{(k)}(\hat{\mathbf{x}}_{\lambda_s}, \lambda_s) + \mathcal{O}(h^{n+2}) \\ &= \frac{\alpha_t}{\sigma_t} \sum_{k=0}^n h^{k+1} \int_0^1 e^{(r-1)h} \frac{r^k}{k!} dr \hat{\mathbf{x}}_\theta^{(k)}(\hat{\mathbf{x}}_{\lambda_s}, \lambda_s) + \mathcal{O}(h^{n+2}) \\ &:= \frac{\alpha_t}{\sigma_t} \sum_{k=0}^n h^{k+1} \psi_{k+1}(h) \hat{\mathbf{x}}_\theta^{(k)}(\hat{\mathbf{x}}_{\lambda_s}, \lambda_s) + \mathcal{O}(h^{n+2}), \end{aligned} \quad (26)$$

where  $\psi_{k+1}(h) = \int_0^1 e^{(r-1)h} \frac{r^k}{k!} dr$  can be computed via the recurrence relation by integration-by-parts formula:

$$\psi_{k+1}(z) = \frac{1}{z} \int_0^1 \frac{r^k}{k!} d e^{(r-1)z} = \frac{1}{z} \left( \frac{1}{k!} - \int_0^1 e^{(r-1)z} \frac{r^{k-1}}{(k-1)!} dr \right) = \frac{1}{z} \left( \frac{1}{k!} - \psi_k(z) \right),$$

and  $\psi_0(z) = e^{-z}$  (Hochbruck & Ostermann, 2005). For example, the closed-forms of  $\psi_k(h)$  for  $k = 1, 2, 3$  are

$$\psi_1(h) = \frac{1 - e^{-h}}{h}, \quad \psi_2(h) = \frac{h - 1 + e^{-h}}{h^2}, \quad \psi_3(h) = \frac{h^2/2 - h + 1 - e^{-h}}{h^3}.$$

**Proof.** In the subsequence analysis, we prove the order of accuracy of UniC for the data prediction model and the result of UniP for the data prediction model follows similarly. Suppose  $\mathbf{x}_t$  is the solution of the diffusion ODE (1). For the data prediction model, define

$$\begin{aligned} \bar{\mathbf{x}}_{t_i} &= \frac{\sigma_{t_i}}{\sigma_{t_{i-1}}} \mathbf{x}_{t_{i-1}} + \alpha_{t_i} (1 - e^{-h_i}) \mathbf{x}_\theta(\mathbf{x}_{t_{i-1}}, t_{i-1}) + \alpha_{t_i} B(h_i) \sum_{m=1}^{p-1} \frac{c_m}{r_m} (\hat{\mathbf{x}}_\theta(\hat{\mathbf{x}}_{\lambda_{s_m}}, \lambda_{s_m}) - \hat{\mathbf{x}}_\theta(\hat{\mathbf{x}}_{\lambda_{t_{i-1}}}, \lambda_{t_{i-1}})) \\ &\quad + \alpha_{t_i} B(h_i) \frac{c_p}{r_p} (\mathbf{x}_\theta(\tilde{\mathbf{x}}_{t_i}, t_i) - \hat{\mathbf{x}}_\theta(\hat{\mathbf{x}}_{\lambda_{t_{i-1}}}, \lambda_{t_{i-1}})). \end{aligned}$$

Similar to (21), since  $\text{Solver-}\mathbf{p}$  has order of accuracy  $p$  and  $B(h) = \mathcal{O}(h)$ , under Assumption D.9, we have  $\bar{\mathbf{x}}_{t_i} = \frac{\sigma_{t_i}}{\sigma_{t_{i-1}}} \mathbf{x}_{t_{i-1}} + \alpha_{t_i} (1 - e^{-h_i}) \mathbf{e}_\theta(\mathbf{x}_{t_{i-1}}, t_{i-1}) + \alpha_{t_i} B(h_i) \sum_{m=1}^p \frac{c_m}{r_m} (\hat{\mathbf{x}}_\theta(\hat{\mathbf{x}}_{\lambda_{s_m}}, \lambda_{s_m}) - \hat{\mathbf{x}}_\theta(\hat{\mathbf{x}}_{\lambda_{t_{i-1}}}, \lambda_{t_{i-1}})) + \mathcal{O}(h^{p+2})$ . Then, the local truncation error on  $t_i$  is given by  $|\mathbf{x}_{t_i} - \bar{\mathbf{x}}_{t_i}|$ . Further, similar to Definition E.1, we shall show that

$$\max_{1 \leq i \leq M} |\mathbf{x}_{t_i} - \bar{\mathbf{x}}_{t_i}| = \mathcal{O}(h^{p+2}), \quad h = \max_{1 \leq i \leq M} h_i.$$

Combining (7) and (26), we have

$$\mathbf{x}_{t_i} = \frac{\sigma_{t_i}}{\sigma_{t_{i-1}}} \mathbf{x}_{t_{i-1}} + \alpha_{t_i} (1 - e^{-h_i}) \mathbf{e}_\theta(\mathbf{x}_{t_{i-1}}, t_{i-1}) + \alpha_{t_i} \sum_{k=1}^p h_i^{k+1} \psi_{k+1}(h_i) \hat{\mathbf{x}}_\theta^{(k)}(\hat{\mathbf{x}}_{\lambda_{t_{i-1}}}, \lambda_{t_{i-1}}) + \mathcal{O}(h^{p+2}).$$

Recall that  $\mathbf{R}_{p,k}^\top$  is the  $k$ -th row of  $\mathbf{R}_p$ . By (11), we have  $|\mathbf{c}_p^\top \mathbf{R}_{p,k}(h_i) - B^{-1}(h_i) h_i^k k! \psi_{k+1}(h_i)| \leq C B^{-1}(h_i) h_i^{p+1}$  for some constant  $C > 0$ . Under Assumption E.3, by Taylor expansion, we obtain

$$\begin{aligned} & \sum_{m=1}^p \frac{c_m}{r_m} (\hat{\mathbf{x}}_\theta(\hat{\mathbf{x}}_{\lambda_{s_m}}, \lambda_{s_m}) - \hat{\mathbf{x}}_\theta(\hat{\mathbf{x}}_{\lambda_{t_{i-1}}}, \lambda_{t_{i-1}})) \\ &= \sum_{n=1}^p \sum_{m=1}^p c_m \frac{r_m^{n-1} h_i^n}{n!} \hat{\mathbf{x}}_\theta^{(n)}(\hat{\mathbf{x}}_{\lambda_{t_{i-1}}}, \lambda_{t_{i-1}}) + \mathcal{O}(h^{p+1}) \\ &= \sum_{n=1}^p \frac{h_i}{n!} \mathbf{c}_p^\top \mathbf{R}_{p,n}(h_i) \hat{\mathbf{x}}_\theta^{(n)}(\hat{\mathbf{x}}_{\lambda_{t_{i-1}}}, \lambda_{t_{i-1}}) + \mathcal{O}(h^{p+1}). \end{aligned}$$

Thus, we have  $\left| \sum_{m=1}^p \frac{c_m}{r_m} (\hat{\mathbf{x}}_\theta(\hat{\mathbf{x}}_{\lambda_{s_m}}, \lambda_{s_m}) - \hat{\mathbf{x}}_\theta(\hat{\mathbf{x}}_{\lambda_{t_{i-1}}}, \lambda_{t_{i-1}})) - B(h_i)^{-1} \sum_{k=1}^p h_i^{k+1} \psi_{k+1}(h_i) \hat{\mathbf{x}}_\theta^{(k)}(\hat{\mathbf{x}}_{\lambda_{t_{i-1}}}, \lambda_{t_{i-1}}) \right| \leq C_1 (B(h_i)^{-1} h_i^{p+2} + h^{p+1})$ . Given  $0 \neq B(h_i) = \mathcal{O}(h_i)$ , we have

$$\begin{aligned} \max_{1 \leq i \leq M} |\mathbf{x}_{t_i} - \bar{\mathbf{x}}_{t_i}| &= \left| \alpha_{t_i} \sum_{k=1}^p h_i^{k+1} \psi_{k+1}(h_i) \hat{\mathbf{x}}_\theta^{(k)}(\hat{\mathbf{x}}_{\lambda_{t_{i-1}}}, \lambda_{t_{i-1}}) \right. \\ &\quad \left. - \alpha_{t_i} B(h_i) \sum_{m=1}^p \frac{c_m}{r_m} (\hat{\mathbf{x}}_\theta(\hat{\mathbf{x}}_{\lambda_{s_m}}, \lambda_{s_m}) - \hat{\mathbf{x}}_\theta(\hat{\mathbf{x}}_{\lambda_{t_{i-1}}}, \lambda_{t_{i-1}})) \right| + \mathcal{O}(h^{p+2}) \\ &= \mathcal{O}(h^{p+2}). \end{aligned}$$

Therefore, UniC- $p$  for the data prediction model is of  $(p+1)$ -th order of accuracy.  $\square$

## E.5. Proof of Theorem C.1

We first give the local truncation error of UniPC $_v$ . Let  $A_{m,n}$  denote the element of  $\mathbf{A}_p$  on row  $m$  and column  $n$ . Define

$$\begin{aligned} \check{\mathbf{x}}_{t_i} &= \frac{\alpha_{t_i}}{\alpha_{t_{i-1}}} \mathbf{x}_{t_{i-1}} - \sigma_{t_i} (e^{h_i} - 1) \mathbf{e}_\theta(\mathbf{x}_{t_{i-1}}, t_{i-1}) \\ &\quad - \sigma_{t_i} \sum_{n=1}^p h_i \varphi_{n+1}(h_i) \sum_{m=1}^{p-1} A_{m,n} (\hat{\mathbf{e}}_\theta(\hat{\mathbf{x}}_{\lambda_{s_m}}, \lambda_{s_m}) - \hat{\mathbf{e}}_\theta(\hat{\mathbf{x}}_{\lambda_{t_{i-1}}}, \lambda_{t_{i-1}})) / r_m \\ &\quad - \sigma_{t_i} \sum_{n=1}^p h_i \varphi_{n+1}(h_i) A_{p,n} (\mathbf{e}_\theta(\check{\mathbf{x}}_{t_i}, t_i) - \hat{\mathbf{e}}_\theta(\hat{\mathbf{x}}_{\lambda_{t_{i-1}}}, \lambda_{t_{i-1}})) / r_p. \end{aligned}$$

Similar to (21), we have

$$\begin{aligned} \check{\mathbf{x}}_{t_i} &= \frac{\alpha_{t_i}}{\alpha_{t_{i-1}}} \mathbf{x}_{t_{i-1}} - \sigma_{t_i} (e^{h_i} - 1) \mathbf{e}_\theta(\mathbf{x}_{t_{i-1}}, t_{i-1}) \\ &\quad - \sigma_{t_i} \sum_{n=1}^p h_i \varphi_{n+1}(h_i) \sum_{m=1}^p A_{m,n} (\hat{\mathbf{e}}_\theta(\hat{\mathbf{x}}_{\lambda_{s_m}}, \lambda_{s_m}) - \hat{\mathbf{e}}_\theta(\hat{\mathbf{x}}_{\lambda_{t_{i-1}}}, \lambda_{t_{i-1}})) / r_m + \mathcal{O}(h^{p+2}). \end{aligned} \quad (27)$$

Suppose  $\mathbf{x}_t$  is the solution of the diffusion ODE (1) and the local truncation error on  $t_i$  is given by  $|\mathbf{x}_{t_i} - \check{\mathbf{x}}_{t_i}|$ . Further, we shall show that the order of accuracy of UniPC<sub>v</sub>- $p$  is  $p+1$ , *i.e.*,

$$\max_{1 \leq i \leq M} |\mathbf{x}_{t_i} - \check{\mathbf{x}}_{t_i}| = \mathcal{O}(h^{p+2}), \quad h = \max_{1 \leq i \leq M} h_i.$$

By (22), we have

$$\mathbf{x}_{t_i} = \frac{\alpha_{t_i}}{\alpha_{t_{i-1}}} \mathbf{x}_{t_{i-1}} - \sigma_{t_i}(e^{h_i} - 1) \boldsymbol{\epsilon}_\theta(\mathbf{x}_{t_{i-1}}, t_{i-1}) - \sigma_{t_i} \sum_{k=1}^p h_i^{k+1} \varphi_{k+1}(h_i) \hat{\boldsymbol{\epsilon}}_\theta^{(k)}(\hat{\mathbf{x}}_{\lambda_{t_{i-1}}}, \lambda_{t_{i-1}}) + \mathcal{O}(h^{p+2}). \quad (28)$$

Under Assumption E.2, by Taylor expansion, we obtain

$$\begin{aligned} & \sum_{k=1}^p h_i \varphi_{k+1}(h_i) \sum_{m=1}^p \frac{A_{m,k}}{r_m} (\hat{\boldsymbol{\epsilon}}_\theta(\hat{\mathbf{x}}_{\lambda_{s_m}}, \lambda_{s_m}) - \hat{\boldsymbol{\epsilon}}_\theta(\hat{\mathbf{x}}_{\lambda_{t_{i-1}}}, \lambda_{t_{i-1}})) \\ &= \sum_{k=1}^p h_i \varphi_{k+1}(h_i) \sum_{m=1}^p A_{m,k} \sum_{n=1}^p \frac{r_m^{n-1} h_i^n}{n!} \hat{\boldsymbol{\epsilon}}_\theta^{(n)}(\hat{\mathbf{x}}_{\lambda_{t_{i-1}}}, \lambda_{t_{i-1}}) + \mathcal{O}(h^{p+2}) \\ &= \sum_{n=1}^p \sum_{k=1}^p \varphi_{k+1}(h_i) \sum_{m=1}^p A_{m,k} \frac{r_m^{n-1} h_i^{n+1}}{n!} \hat{\boldsymbol{\epsilon}}_\theta^{(n)}(\hat{\mathbf{x}}_{\lambda_{t_{i-1}}}, \lambda_{t_{i-1}}) + \mathcal{O}(h^{p+2}) \\ &= \sum_{n=1}^p \sum_{k=1}^p \varphi_{k+1}(h_i) h_i^{n+1} (1(k=n) + \mathcal{O}(h^p)) \hat{\boldsymbol{\epsilon}}_\theta^{(n)}(\hat{\mathbf{x}}_{\lambda_{t_{i-1}}}, \lambda_{t_{i-1}}) + \mathcal{O}(h^{p+2}) \\ &= \sum_{n=1}^p h_i^{n+1} \varphi_{n+1}(h_i) \hat{\boldsymbol{\epsilon}}_\theta^{(n)}(\hat{\mathbf{x}}_{\lambda_{t_{i-1}}}, \lambda_{t_{i-1}}) + \mathcal{O}(h^{p+2}). \end{aligned}$$

Thus, we have

$$\max_{1 \leq i \leq M} |\mathbf{x}_{t_i} - \check{\mathbf{x}}_{t_i}| = \mathcal{O}(h^{p+2}).$$

Therefore, UniPC<sub>v</sub>- $p$  is of  $(p+1)$ -th order of accuracy.  $\square$

## E.6. Proof of Proposition D.5

For UniP- $p$ , we define

$$\bar{\mathbf{x}}_{t_i} = \frac{\alpha_{t_i}}{\alpha_{t_{i-1}}} \mathbf{x}_{t_{i-1}} - \sigma_{t_i}(e^{h_i} - 1) \boldsymbol{\epsilon}_\theta(\mathbf{x}_{t_{i-1}}, t_{i-1}) - \sigma_{t_i} B(h_i) \sum_{m=1}^{p-1} \frac{a_m}{r_m} (\hat{\boldsymbol{\epsilon}}_\theta(\hat{\mathbf{x}}_{\lambda_{s_m}}, \lambda_{s_m}) - \hat{\boldsymbol{\epsilon}}_\theta(\hat{\mathbf{x}}_{\lambda_{t_{i-1}}}, \lambda_{t_{i-1}})). \quad (29)$$

By Assumption D.2, we have  $|\boldsymbol{\epsilon}_\theta(\tilde{\mathbf{x}}_s, s) - \boldsymbol{\epsilon}_\theta(\mathbf{x}_s, s)| \leq L |\tilde{\mathbf{x}}_s - \mathbf{x}_s|$ . Therefore, for sufficiently large constants  $C, C_1 > 0$  depending on  $\{a_m\}$  and  $\{r_m\}$ , we have

$$|\tilde{\mathbf{x}}_{t_i} - \bar{\mathbf{x}}_{t_i}| \leq \left( \frac{\alpha_{t_i}}{\alpha_{t_{i-1}}} + L \sigma_{t_i}(e^{h_i} - 1) + CLph \right) |\tilde{\mathbf{x}}_{t_{i-1}} - \mathbf{x}_{t_{i-1}}| + CLh \sum_{m=1}^{p-1} |\tilde{\mathbf{x}}_{t_{i-m-1}} - \mathbf{x}_{t_{i-m-1}}|. \quad (30)$$

For simplicity, define  $e_i = |\tilde{\mathbf{x}}_{t_i} - \mathbf{x}_{t_i}|$ ,  $f_n = \max_{0 \leq i \leq n} |e_i|$ . Using Theorem 3.1 and (30), we obtain

$$e_i \leq \left( \frac{\alpha_{t_i}}{\alpha_{t_{i-1}}} + L \sigma_{t_i}(e^{h_i} - 1) + CLph \right) e_{i-1} + CLh \sum_{m=1}^{p-1} e_{i-1-m} + C_0 h^{p+1}. \quad (31)$$

Let  $\beta_i := \frac{\alpha_{t_i}}{\alpha_{t_{i-1}}} + L \sigma_{t_i}(e^{h_i} - 1) + CLph$ . Then, it follows that

$$e_i \leq (CLph + \beta_i) f_{i-1} + C_0 h^{p+1}.$$

Since  $\beta_i + CLph > 1$  for sufficiently small  $h$ , the right hand side is also a trivial bound for  $f_{i-1}$ , because  $\alpha_t > 0$  is monotone decreasing thus  $\alpha_{t_i} < \alpha_{t_{i-1}}$ . We then have

$$f_i \leq (CLph + \beta_i) f_{i-1} + C_0 h^{p+1}. \quad (32)$$

Let  $\sigma := \max_{1 \leq i \leq M} \sigma_{t_i} + 2Cp$ . By elementary calculation, under Assumption D.3 we have

$$\prod_{i=p}^M (\beta_i + CLph) \leq C_1 \prod_{i=p}^M (\alpha_{t_i}/\alpha_{t_{i-1}} + L\sigma/M) = C_1 \frac{\alpha_{t_M}}{\alpha_{t_{p-1}}} \prod_{i=p}^M \left(1 + \frac{L\sigma\alpha_{t_{i-1}}}{\alpha_{t_i} M}\right) \leq C_2 e^{b\sigma}, \quad (33)$$

where  $C_1, C_2$  are sufficiently large constants. Under Assumption D.4 with  $k = p$ ,  $f_{p-1} = \max_{0 \leq i \leq p-1} |\tilde{\mathbf{x}}_{t_i} - \mathbf{x}_{t_i}| \leq c_0 h^p$ . Repeat the argument of (32), under Assumption D.3 by (33), there exists constant  $C_3, C_4 > 0$  such that

$$f_M \leq C_2 e^{b\sigma} f_{p-1} + C_3 M h^{p+1} \leq C_4 h^p. \quad (34)$$

Therefore, the convergence order of UniP- $p$  is  $p$ .  $\square$

### E.7. Proof of Proposition D.6

For the sake of clarity, we use  $\bar{\mathbf{x}}_{t_i}^c = \frac{\alpha_{t_i}}{\alpha_{t_{i-1}}} \mathbf{x}_{t_{i-1}} - \sigma_{t_i} (e^{h_i} - 1) \epsilon_\theta(\mathbf{x}_{t_{i-1}}, t_{i-1}) - \sigma_{t_i} B(h_i) \sum_{m=1}^p \frac{a_m}{r_m} (\hat{\epsilon}_\theta(\hat{\mathbf{x}}_{\lambda_{s_m}}, \lambda_{s_m}) - \hat{\epsilon}_\theta(\hat{\mathbf{x}}_{\lambda_{t_{i-1}}}, \lambda_{t_{i-1}}))$  for UniC- $p$  and use  $\bar{\mathbf{x}}_{t_i}$  of (29) for UniP- $p$ . Similar to (30), we have for  $i \geq p$ ,

$$\begin{aligned} |\tilde{\mathbf{x}}_{t_i}^c - \bar{\mathbf{x}}_{t_i}^c| &\leq \left( \frac{\alpha_{t_i}}{\alpha_{t_{i-1}}} + L\sigma_{t_i} (e^{h_i} - 1) + CLph \right) |\tilde{\mathbf{x}}_{t_{i-1}}^c - \mathbf{x}_{t_{i-1}}| \\ &\quad + CLh \sum_{m=1}^{p-1} |\tilde{\mathbf{x}}_{t_{i-m-1}}^c - \mathbf{x}_{t_{i-m-1}}| + LhC_1 |\tilde{\mathbf{x}}_{t_i} - \mathbf{x}_{t_i}|, \end{aligned} \quad (35)$$

where for the oracle UniPC (see Section 4.2 for definition), the UniP- $p$  admits

$$\begin{aligned} |\tilde{\mathbf{x}}_{t_i} - \bar{\mathbf{x}}_{t_i}| &\leq \left( \frac{\alpha_{t_i}}{\alpha_{t_{i-1}}} + L\sigma_{t_i} (e^{h_i} - 1) + CLph \right) |\tilde{\mathbf{x}}_{t_{i-1}}^c - \mathbf{x}_{t_{i-1}}| \\ &\quad + CLh \sum_{m=1}^{p-1} |\tilde{\mathbf{x}}_{t_{i-m-1}}^c - \mathbf{x}_{t_{i-m-1}}|. \end{aligned} \quad (36)$$

Define  $e_i^c = |\tilde{\mathbf{x}}_{t_i}^c - \mathbf{x}_{t_i}|$ ,  $f_n^c = \max_{0 \leq i \leq n} |e_i^c|$ . Write  $\beta_i := \frac{\alpha_{t_i}}{\alpha_{t_{i-1}}} + L\sigma_{t_i} (e^{h_i} - 1) + CLph$ . Let  $\sigma := \max_{1 \leq i \leq M} \sigma_{t_i} + 2Cp$ . As shown in the proof of Theorem 3.1,  $|\mathbf{x}_{t_i} - \bar{\mathbf{x}}_{t_i}^c| = \mathcal{O}(h^{p+2})$ . Combining the local truncation error, it follows that

$$\begin{aligned} f_i^c &\leq \beta_i f_{i-1}^c + CLhp f_{i-1}^c + LhC_1 (\beta_i f_{i-1}^c + CLhp f_{i-1}^c + C_2 h^{p+1}) + C_0 h^{p+2} \\ &\leq (1 + LhC_1) (\beta_i + CLhp) f_{i-1}^c + C_2 LC_1 h^{p+2} + C_0 h^{p+2}. \end{aligned}$$

Repeating this argument, similar to (34), we have

$$\begin{aligned} |\tilde{\mathbf{x}}_{t_M}^c - \mathbf{x}_0| &\leq f_M^c \leq \prod_{i=p}^M (1 + LhC_1) (\beta_i + CLhp) f_{p-1}^c + MC_2 h^{p+2} \\ &\leq C_3 e^{LC_1 + b\sigma} f_{p-1}^c + MC_2 h^{p+2}. \end{aligned} \quad (37)$$

For  $0 \leq i < p$ , we have

$$\begin{aligned} |\tilde{\mathbf{x}}_{t_i}^c - \bar{\mathbf{x}}_{t_i}| &\leq \left( \frac{\alpha_{t_i}}{\alpha_{t_{i-1}}} + L\sigma_{t_i} (e^{h_i} - 1) + CLph \right) |\tilde{\mathbf{x}}_{t_{i-1}}^c - \mathbf{x}_{t_{i-1}}| \\ &\quad + CLh \sum_{m=1}^{i-1} |\tilde{\mathbf{x}}_{t_{i-m-1}}^c - \mathbf{x}_{t_{i-m-1}}| + LhC_1 |\tilde{\mathbf{x}}_{t_i} - \mathbf{x}_{t_i}|. \end{aligned}$$

Therefore, under Assumption D.4 with  $k = p$ , we have for  $0 \leq i \leq p - 1$

$$f_i^c \leq \beta_i f_{i-1}^c + c_0 CLph^{p+1} + Lh^{p+1}c_0C_1.$$

Repeat this argument, we find for a constant  $C_4 > 0$

$$f_{p-1}^c \leq C_4 h^{p+1}. \quad (38)$$

Combining (37) and (38), we have

$$|\tilde{\mathbf{x}}_{t_M}^c - \mathbf{x}_0| = \mathcal{O}(h^{p+1}).$$

For the non-oracle solver, for the step of UniP- $p$  we have :

$$\begin{aligned} |\tilde{\mathbf{x}}_{t_i} - \mathbf{x}_{t_i}| &\leq \frac{\alpha_{t_i}}{\alpha_{t_{i-1}}} |\tilde{\mathbf{x}}_{t_{i-1}}^c - \mathbf{x}_{t_{i-1}}| + (CLph + L\sigma_{t_i}(e^{h_i} - 1)) |\tilde{\mathbf{x}}_{t_{i-1}} - \mathbf{x}_{t_{i-1}}| \\ &+ CLh \sum_{m=1}^{p-1} |\tilde{\mathbf{x}}_{t_{i-m-1}} - \mathbf{x}_{t_{i-m-1}}| + C_2 h^{p+1}. \end{aligned} \quad (39)$$

Let  $e_n = |\tilde{\mathbf{x}}_{t_n} - \mathbf{x}_{t_n}|$ ,  $f_i = \max_{1 \leq i \leq n} e_i$ . Under Assumption D.4 with  $k = p$ ,  $f_{p-1} \leq c_0 h^p$ . For  $0 \leq i < p$ , we have

$$\begin{aligned} |\tilde{\mathbf{x}}_{t_i}^c - \mathbf{x}_{t_i}| &\leq \frac{\alpha_{t_i}}{\alpha_{t_{i-1}}} |\tilde{\mathbf{x}}_{t_{i-1}}^c - \mathbf{x}_{t_{i-1}}| + (CLph + L\sigma_{t_i}(e^{h_i} - 1)) |\tilde{\mathbf{x}}_{t_{i-1}} - \mathbf{x}_{t_{i-1}}| \\ &+ CLh \sum_{m=1}^{i-1} |\tilde{\mathbf{x}}_{t_{i-m-1}} - \mathbf{x}_{t_{i-m-1}}| + LhC_1 |\tilde{\mathbf{x}}_{t_i} - \mathbf{x}_{t_i}| + C_0 h^{p+2}. \end{aligned}$$

Similar to (38), we obtain  $f_{p-1}^c = \mathcal{O}(h^{p+1})$ . Iterating (35) and (39), by Theorem 3.1 we have  $|\tilde{\mathbf{x}}_{t_M}^c - \mathbf{x}_0| = \mathcal{O}(h^{p+1})$ .  $\square$

## F. Implementation Details

We now provide more details about our UniPC and the experiments.

### F.1. Implementation Details about UniPC

Our UniPC is implemented in a multistep manner by default, as is illustrated in Figure 1 and Algorithm 5,6. In this case, the extra timesteps that are used to obtain the estimation of higher-order derivatives  $\{s_m\}_{m=1}^{p-1}$  are set to be larger than  $t_{i-1}$ . In other words,  $\{r_m\}_{m=1}^{p-1}$  are all negative. We have also found that the conditions of UniP-2 and UniC-1 degenerate to a simple equation where only a single  $a_1$  is unknown. Specifically, considering (6) and (5), we find that

$$a_1 B(h) - \psi_1(h) = \mathcal{O}(h^2), \quad (40)$$

where

$$\psi_1(h) = h\varphi_2(h) = \frac{e^h - h - 1}{h} = \frac{1}{2}h + \mathcal{O}(h^2). \quad (41)$$

For  $B_1(h) = h$ , it is easy to show that when  $a_1 = 0.5$ ,

$$a_1 B(h) - \psi_1(h) = \frac{1}{2}h - \frac{1}{2}h + \mathcal{O}(h^2) = \mathcal{O}(h^2). \quad (42)$$

For  $B_2(h) = e^h - 1 = h + \mathcal{O}(h^2)$ , the derivation is similar and  $a_1 = 1/2$  also satisfies the condition. Therefore, we can directly set  $a_1 = 1/2$  for UniP-2 and UniC-1 without solving the equation. For higher orders, the vector  $\mathbf{a}_p$  is computed normally through the inverse of the  $\mathbf{R}_p$  matrix.

To provide enough data points for high-order UniPC, we need a warming-up procedure in the first few steps, as is also used in previous multistep approaches (Lu et al., 2022b) and is shown in Algorithm 5,6,. Since our UniC needs to compute  $\epsilon_\theta(\tilde{\mathbf{x}}_{t_i}, t_i)$ , *i.e.*, the model output at the current timestep  $t_i$  to obtain the corrected result  $\mathbf{x}_{t_i}^c$ , performing our UniC at the last sampling step will introduce an extra function evaluation. Therefore, we do not use the corrector after the last execution of the predictor for fair comparisons.

Table 6. More unconditional sampling results on CIFAR10 (Krizhevsky et al., 2009).

Sampling Method	NFE					
	5	6	7	8	9	10
DDIM (Song et al., 2021a)	55.04	41.81	33.10	27.54	22.92	20.02
DDIM + UniC-1	47.22	33.70	24.60	19.20	15.33	12.77
DPM-Solver-3 (Lu et al., 2022a)	290.65	23.91	15.06	23.56	5.65	4.64
DPM-Solver++(2M) (Lu et al., 2022b)	33.86	21.12	13.93	10.24	7.97	6.83
DPM-Solver++(2M) + UniC-2	31.23	17.96	11.23	8.09	6.29	5.51
DPM-Solver++(3M) (Lu et al., 2022b)	29.22	13.28	7.18	5.21	4.40	4.03
DPM-Solver++(3M) + UniC-3	25.50	11.72	6.79	5.04	4.22	3.90
UniPC-3- $B_1(h)$	<b>23.22</b>	<b>10.33</b>	6.41	5.10	4.29	3.97
UniPC-3- $B_2(h)$	26.20	11.48	6.73	5.11	4.30	<b>3.87</b>
UniPC <sub>v</sub> -3	25.60	11.10	<b>6.18</b>	<b>4.80</b>	<b>4.19</b>	4.18

Table 7. More unconditional sampling results on FFHQ (Karras et al., 2019).

Sampling Method	NFE					
	5	6	7	8	9	10
DDIM (Song et al., 2021a)	58.23	44.40	34.52	28.06	23.52	19.72
DDIM + UniC	39.41	26.48	18.58	14.56	11.97	10.33
DPM-Solver-3 (Lu et al., 2022a)	54.17	25.24	12.37	8.06	10.22	7.74
DPM-Solver++(2M) (Lu et al., 2022b)	32.50	20.32	14.25	11.30	9.45	8.28
DPM-Solver++(2M) + UniC	24.20	14.92	10.82	9.11	8.01	7.39
DPM-Solver++(3M) (Lu et al., 2022b)	27.15	15.60	10.81	8.98	7.89	7.39
DPM-Solver++(3M) + UniC	21.73	13.38	10.06	8.67	7.89	7.22
UniPC-3- $B_1(h)$	<b>18.66</b>	<b>11.89</b>	<b>9.51</b>	<b>8.21</b>	<b>7.62</b>	<b>6.99</b>
UniPC-3- $B_2(h)$	21.66	13.21	9.93	8.63	7.69	7.20

## F.2. Details about the experiments.

We now provide more details of our experiments. For unconditional sampling on CIFAR10 (Krizhevsky et al., 2009), we use the ScoreSDE (Song et al., 2021b) codebase and their pre-trained model, which is a continuous-time DDPM++ model (Song et al., 2021b). More concretely, we use the `cifar10_ddpmpp_deep_continuous` config file, the same as the example provided by the official code of DPM-Solver (Lu et al., 2022a). To compute FID, we adopt the statistic file provided by ScoreSDE (Song et al., 2021b) codebase. For unconditional sampling on LSUN Bedroom (Yu et al., 2015) and FFHQ (Karras et al., 2019), we adopt the latent-space DPM provided by the stable-diffusion codebase (Rombach et al., 2022). Since there is no statistic file for these two datasets in the codebase, we compute the dataset statistic of FFHQ using the script in the library `pytorch-fid`, and borrow the statistic file of LSUN Bedroom from the guided-diffusion codebase (Dhariwal & Nichol, 2021). For conditional sampling on pixel space, we implement our method in guided-diffusion codebase (Dhariwal & Nichol, 2021) and use the pre-trained checkpoint for ImageNet 256×256. For conditional sampling on latent space, we adopt the stable-diffusion codebase and use their `sd-v1-3.ckpt` checkpoint, which is pre-trained on LAION (Schuhmann et al., 2021). To obtain the text prompts, we randomly sample 10K captions from the MS-COCO2014 validation dataset (Lin et al., 2014). We sample 10K random latent code  $\mathbf{x}_T^*$  for each caption and fix them when using different methods.

## G. More Results

In this section, we will provide more detailed results, including both quantitative and qualitative results.

### G.1. More Quantitative Results

We start by demonstrating detailed results on CIFAR10 (Krizhevsky et al., 2009), which are shown in Table 6. The results of our proposed method are highlighted in gray. Apart from the results already illustrated in Figure 3, we also include the

Table 8. More unconditional results on LSUN (Yu et al., 2015).

Sampling Method	NFE					
	5	6	7	8	9	10
DDIM (Song et al., 2021a)	40.40	25.56	17.93	13.47	10.77	8.95
DPM-Solver++(3M) (Lu et al., 2022b)	17.79	8.03	4.97	4.04	3.79	3.63
DPM-Solver++(3M) + UniC	13.79	6.53	4.58	3.98	3.69	<b>3.52</b>
UniPC-3- $B_1(h)$	<b>11.88</b>	<b>5.99</b>	<b>4.40</b>	<b>3.97</b>	<b>3.74</b>	3.62
UniPC-3- $B_2(h)$	13.60	6.44	4.47	3.91	3.76	3.54

Table 9. More conditional sampling results on ImageNet 256×256.

Sampling Method	NFE					
	5	6	7	8	9	10
<i>guidance scale s = 8.0</i>						
DDIM (Song et al., 2021a)	38.11	25.31	17.71	14.50	11.51	10.34
DEIS (Zhang & Chen, 2022)	83.80	67.73	54.91	44.91	37.84	31.84
DPM-Solver++ (Lu et al., 2022b)	55.64	24.07	14.25	12.22	9.53	8.49
UniPC- $B_1(h)$	68.69	34.76	22.79	20.45	17.44	16.02
UniPC- $B_2(h)$	<b>25.87</b>	<b>12.30</b>	<b>8.72</b>	<b>8.68</b>	<b>7.72</b>	<b>7.51</b>
<i>guidance scale s = 4.0</i>						
DDIM (Song et al., 2021a)	27.41	18.47	13.52	11.19	9.66	8.76
DEIS (Zhang & Chen, 2022)	37.86	24.00	16.00	11.69	9.49	8.05
DPM-Solver++ (Lu et al., 2022b)	31.57	14.58	9.92	9.43	7.98	7.51
UniPC- $B_1(h)$	22.83	12.59	9.77	9.67	8.90	8.52
UniPC- $B_2(h)$	<b>19.48</b>	<b>10.81</b>	<b>8.18</b>	<b>8.09</b>	<b>7.49</b>	<b>7.31</b>
<i>guidance scale s = 1.0</i>						
DDIM (Song et al., 2021a)	36.08	27.02	21.38	17.59	15.20	13.40
DPM-Solver++ (Lu et al., 2022b)	26.10	17.75	13.95	13.10	11.88	11.11
UniPC- $B_2(h)$	<b>22.22</b>	<b>15.79</b>	<b>12.72</b>	<b>12.28</b>	<b>11.30</b>	<b>10.84</b>

performance of the DPM-Solver (Lu et al., 2022a) and our UniPC<sub>v</sub>, which has varying coefficients (see Appendix C for detailed description). Firstly, we show that DPM-Solver performs very unstable with extremely few steps: the FID of 5 NFE comes to 290.65, which means the solver crashes in this case. Besides, we also show that the DPM-Solver++(3M) (Lu et al., 2022b) performs consistently better than DPM-Solver-3 (Lu et al., 2022a), indicating the multistep method is more effective in few-step sampling setting. That is also why we tend to use DPM-Solver++ as our baseline method in all of our experiments. Table 6 also shows the comparisons between variants of our UniPC, such as UniPC with different instantiations of  $B(h)$  and UniPC<sub>v</sub>. Since the comparisons between  $B_1(h)$  and  $B_2(h)$  have already been discussed in Section 4.2, we now focus on the analysis of the performance of UniPC<sub>v</sub>. We find UniPC<sub>v</sub> achieves the best sampling quality with 7 9 NFE, while cannot beat other variants of UniPC with 5,6,10 NFE. These results show that different variants of our UniPC may have different applications and we should select the most suitable one according to the budget of NFE. We also include more experimental results of the unconditional sampling results on FFHQ (Karras et al., 2019) in LSUN Bedroom (Yu et al., 2015), as summarized in Table 7 and Table 8. Note that there are fewer results for LSUN because we performed most of our experiments on FFHQ and CIFAR10 in the early stage. Nevertheless, the overall conclusions of the results on different datasets are aligned. To sum up, our results show (1) multistep methods behave better than singlestep ones when the NFE budget is extremely small. (2) our UniC can consistently improve the sampling quality of a wide range of off-the-shelf solvers. (3) selecting a proper variant of UniPC can yield better results in most cases.

We also provide more results on guided sampling on ImageNet 256×256, as is shown in Table 9. We evaluate the performance of DEIS (Zhang & Chen, 2022) and find it performs worse than both the DPM-Solver++ and our UniPC.

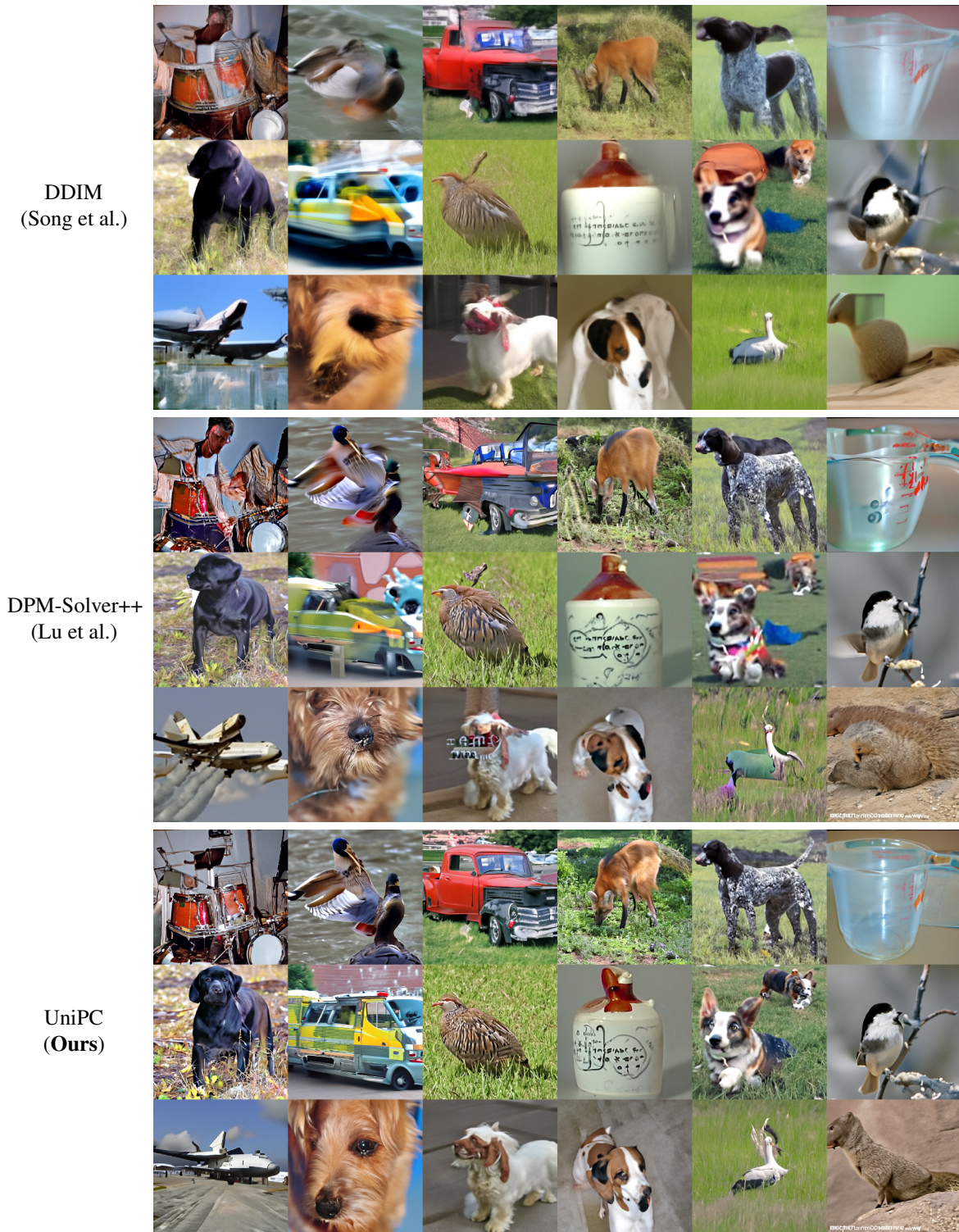


Figure 5. Comparisons between the images sampled from a DPM pre-trained on ImageNet256  $\times$  256 using DDIM (Song et al., 2021a), DPM-Solver++ (Lu et al., 2022b) and our UniPC with only 7 NFE.

Besides, we have compared the choice of  $B(h)$  on guided sampling, where we find  $B_2(h)$  significantly outperforms  $B_1(h)$ , perhaps because  $B_1(h) = h$  is too simple and not suitable for the guided sampling. We have also added the results when the guidance scale  $s = 1.0$ . The results show that our method can achieve better sampling quality with both large and small guidance scales with few sampling steps.

Text Prompts	DDIM (Song et al., 2021a)	DPM-Solver++ (Lu et al., 2022b)	UniPC (Ours)
<i>“A bear extends its long tongue while yawning.”</i>			
<i>“A bedroom with a bed that has a blue and white striped comforter.”</i>			
<i>“A pan of pizza with toppings on a table.”</i>			
<i>“A couple of guys that are eating some food.”</i>			

Figure 6. Comparisons of text-to-image results among UniPC, DDIM (Song et al., 2021a) and DPM-Solver++ (Lu et al., 2022b). Images are sampled using only 5 NFE.

## G.2. More Qualitative Results

We provide more visualizations to demonstrate the qualitative performance. First, we consider the class-conditioned guided sampling, *i.e.*, the conditional sampling on ImageNet (Deng et al., 2009) in Figure 5. Specifically, we compare the sampling quality of each method with only 7 NFE. Note that we randomly sample the class from the total 1000 classes in ImageNet for each image sample, but fix the initial noise for different methods. We also evaluate our method on the prevalent text-to-image model in stable-diffusion (Rombach et al., 2022) and the results are demonstrated in Figure 6. The images are sampled with the corresponding text prompts as the guidance using only 5 NFE. These comparisons clearly show that our UniPC generates more plausible images than both DDIM (Nichol & Dhariwal, 2021) and DPM-Solver++ (Lu et al., 2022b).